PSD NORTH AMERICA
Power Systems Design: Empowering Global Innovation

July/August 2012

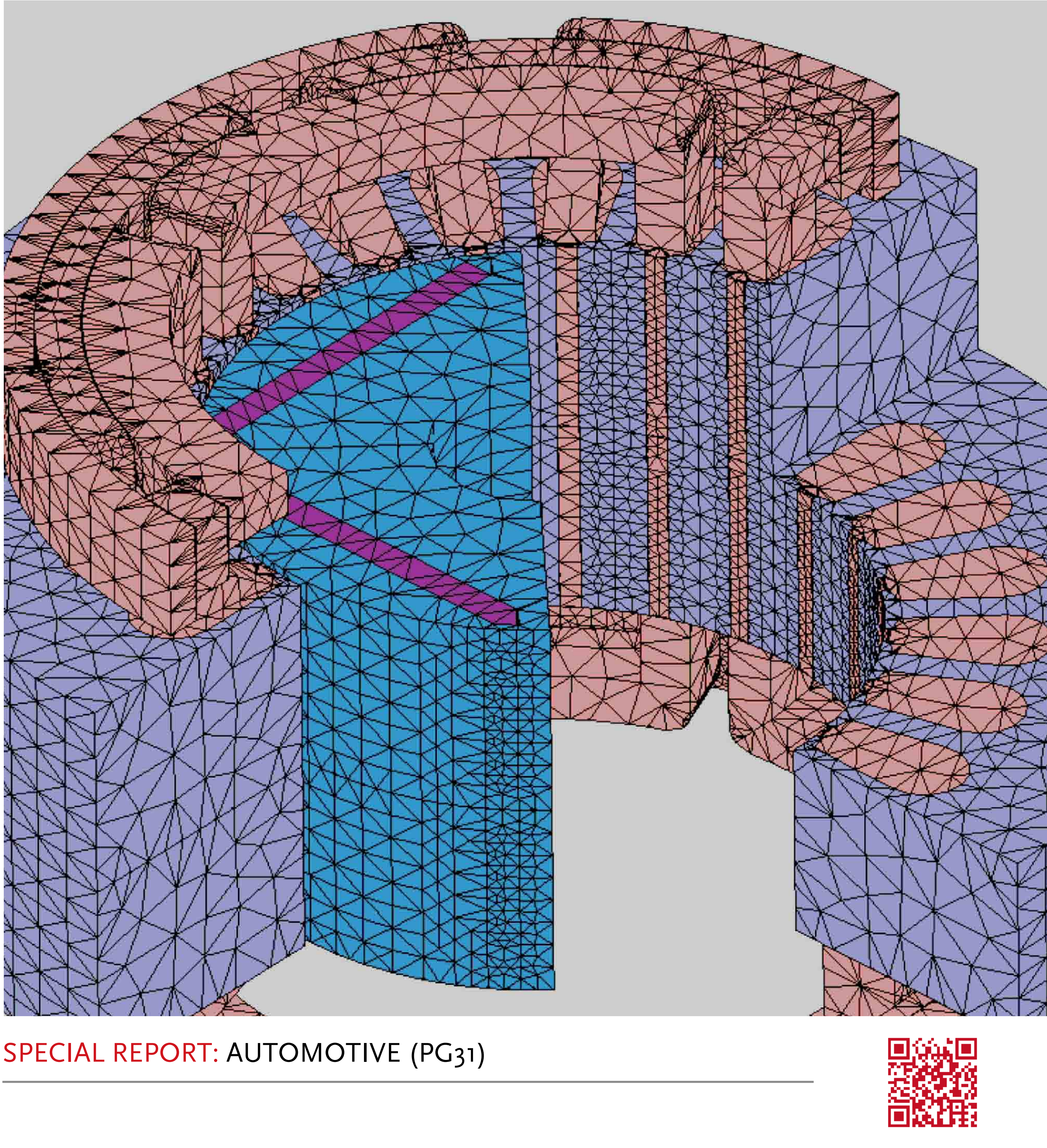

SPECIAL REPORT: AUTOMOTIVE (PG31)

PSD NORTH AMERICA
Power Systems Design: Empowering Global Innovation

WWW.POWERSYSTEMSDESIGN.COM

Visit us online for exclusive content; Industry News, Products, Reviews, and full PSD archives and back issues

2 **VIEWpoint**
The Current Response
By Joshua Israelsohn, Editor-in-Chief, Power Systems Design

4 **POWERline**
ZVS POLs provide 98% pk η and voltage ratios to 36:1

6 **POWERplayer**
PCB Layout for Accurate Current Sensing
By Kory Schroeder, Stackpole Electronics

8 **MARKETwatch**
Power ICs Driving Forward in Automotive Electronics
By Ben Scott, IMS Research

9 **DESIGNtips**
Audiosusceptibility Measurements and Loop Gains,
By Dr. Ray Ridley, Ridley Engineering

COVER STORY

14 **Improving Electric-Motor Testing Techniques**
By Nick Keel, Product Manager, Veristand National Instruments & Frank Heidemann, CEO, Set GmbH

TECHNICAL FEATURES

18 **Power Supplies**
Reduce Stand-By Power Loss in AC—DC Supplies
By Scott Brown, iWatt

22 **Packaging**
Estimating Bond Wire Current-Carrying Capacity
By Jitesh Shah, IDT

26 **Power Supplies**
Improve Set-Top-Box Supply Efficiency
By Yong Ang, Diodes

SPECIAL REPORT: AUTOMOTIVE

32 **Sleeping Conserves Energy**
By Fritz Burkhardt, ST Microelectronics

36 **Hall-Effect Current Sensing in HEVs and EVs**
By Shaun Milan, Michael Doogue, Georges El Bacha, Allegro MicroSystems

39 **High-Side Automotive Battery Monitoring**
By Manfred Brandl, ams AG

42 **Current Sensing in an Automotive Environment**
By Warren Pettigrew, Raztec

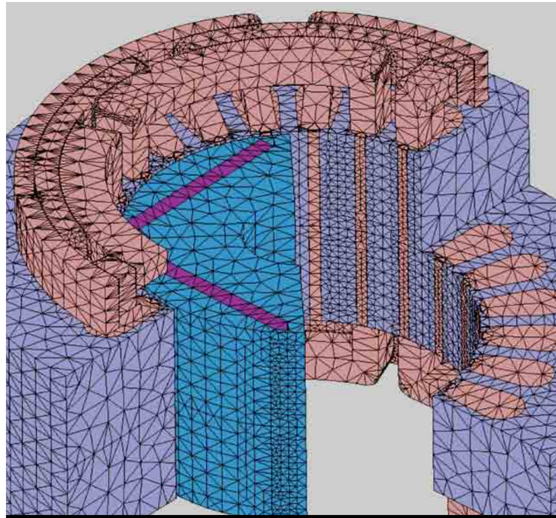

COVER STORY
Improving Electric-Motor Testing Techniques (pg 14)

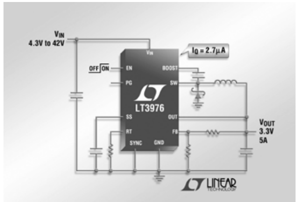

Highlighted Products News, Industry News and more web-only content, to:
www.powersystemsdesign.com

46 **CAREERdevelopment**
Vehicle Electrification Sparks Engineering Demand
By David G. Morrison, Editor, How2Power.com

52 **GREENpage**
Cometh the Hour, Cometh the Man
Reported By Gail Purvis, Europe Editor, Power Systems Design

52 **Dilbert**

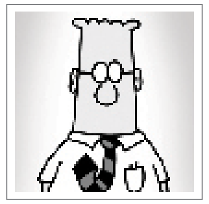

PSD NORTH AMERICA

AGS Media Group
146 Charles Street
Annapolis, MD 21401 USATel: +410.295.0177
Fax: +510.217.3608
www.powersystemsdesign.com

Editor-in-Chief
Joshua Israelsohn, Editor-in-Chief, Power Systems Design
joshua@powersystemsdesign.com

Contributing Editors
Gail Purvis, European Editor, Power Systems Design
Gail.Purvis@powersystemsdesign.com

Liu Hong, Editor-in-Chief, Power Systems Design China
powersdc@126.com

Ash Sharma, IMS Research
Ash.sharma@imsresearch.com

Dr. Ray Ridley, Ridley *Engineering*
RRidley@ridleyengineerng.com

David Morrison, How2Power
david@how2power.com

Publishing Director
Jim Graham
jim.graham@powersystemsdesign.com

Publisher
Julia Stocks
Julia.stocks@powersystemsdesign.com

Circulation Management
Kathryn Philips
Kathryn.phillips@powersystemsdesign.com

Magazine Design
Louis C. Geiger
louis@agencyofrecord.com

Production Manager
Chris Corneal
chris.corneal@powersystemsdesign.com

Registration of copyright: January 2004
ISSN number: 1613-6365

Volume 4, Issue 4

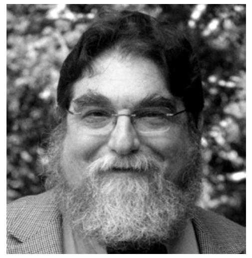

THE CURRENT RESPONSE

I recalled in print some years ago that the first car I ever drove had precisely two electric motors: One was the starter and the other drove the heater fan. Even the windshield wipers operated by non-electric means, depending on manifold vacuum tapped at the engine intake. That vehicle came to mind at that time because, those many years later, I then recently sat around a table with a couple of automotive electronics designers and we tallied up no fewer than 50 applications for motors or electromagnetic actuators in the cars of the day.

Today the impressive evolution isn't so much in the increasing number of roles motors can play in a vehicle, though relatively new ones such as electric traction drives—either as primary or secondary sources of drive-train energy—are certainly of keen interest as are the many efforts to get traditionally hydraulic systems off the belt. What seems to be of greater concern amongst the automotive electronics suppliers to whom we've been listening is the efficient use and management of electric power throughout the vehicle—be it to drive a motor, operate a communication bus, light an LED, or charge a battery.

Current measurement is a key topic for many automotive suppliers and this month's issue reflects that with several articles that take on various aspects of that subject. Seemingly simple, it turns out that substantial engineering goes into making high-quality current measurements in the automotive environment. Such measurements occur over a surprisingly large dynamic range—five orders of magnitude—and, there alone, may well outstrip any other under-hood monitored quantity. The number of technologies that can apply to making such measurements, or at least a subrange thereof, are numerous as are the applications for the data.

We amassed, in fact, more articles for this issue than the magazine can fit. After enjoying this month's issue, you can read the others on our website, www.powersystemsdesign.com, where you'll also find a host of other technical information.

Happy motoring!

Joshua Israelsohn

Editor-in-Chief
Power Systems Design
joshua@powersystemsdesign.com

ZVS POLS PROVIDE 98% PK η AND VOLTAGE RATIOS TO 36:1

A new series of ZVS (zero-voltage switching) buck POL regulators afford board-level designers high power density and high ease of use.

Vicor's new Picor PI33XX ZVS buck regulator series provides power efficiency up to 98% peak and supports outputs to 10 A per package in a high-density 10 x 14 x 2.56 mm LGA package (Figure 1). Products in the PI33XX series are highly integrated with control circuitry, power semiconductors, and support components, requiring only input and output ceramic capacitors and an output inductor. No frequency compensation, parametric settings, or incremental external components are necessary.

PI33XX buck regulators can convert input supplies ranging from 8V to 36V to output voltages from 1V to 16V for power delivery up to 120W. Board designers can further increase power delivery by interleaving up to six PI33XX buck regulators using single wire current sharing without the need of any additional components.

The use of a ZVS topology enables high-frequency operation that maximizes efficiency by minimizing the significant switching losses associated with conventional buck regulators that use hard-switching topologies. The PI33XX series' high switching frequency also reduces the size of the external filtering components, improving power density while enabling fast dynamic response to line and load transients. The PI33XX series sustains high switching frequency all the way up to the rated input voltage without sacrificing efficiency and, with its 20ns minimum on time, supports large step down conversions up to 36:1.

Part Number	Output Voltage	Margining Range	I_{OUT} Max
PI3311-00-LGIZ	1.0 V	1.0 – 1.4 V	10 A
PI3312-00-LGIZ	2.5 V	2.0 – 3.1 V	10 A
PI3301-00-LGIZ	3.3 V	2.3 – 4.1 V	10 A
PI3302-00-LGIZ	5.0 V	3.3 – 6.5 V	10 A
PI3303-00-LGIZ	12 V	6.5 – 13.0 V	8 A
PI3305-00-LGIZ	15 V	10.0 – 16.0 V	8 A

Table 1

A wide operating temperature range of -40 to +125 °C allows for use in almost any environment. A compact 266 mm2 total footprint, including all necessary external passives, frees up valuable PCB real-estate for your densest designs.

Picor PI33XX ZVS buck regulators also offer an optional I2C extended fault telemetry capability allowing for six distinct types of fault reporting including over-temperature, over-current, output-voltage high, input over-voltage, input under-voltage, and controller-VCC under-voltage. Additional device-programmable I2C features include margining, enable pin logic polarity, and phase delay.

The initial release includes six models priced at $12.85 (1000)

www.vicr.com

PCB LAYOUT FOR ACCURATE CURRENT SENSING

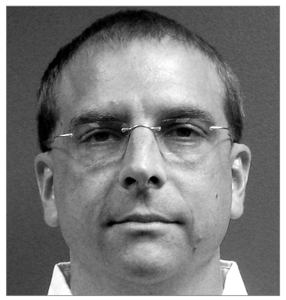

By: Kory Schroeder

Stackpole Electronics recently announced its 5 W ultra-precision current-sensing resistor—the CSS4527—available in values between 0.5 and 120 mΩ with tolerances to 0.5% and 50 ppm/°C TCR.

Observing that these current-sense resistors offered no Kelvin terminals, Power Systems Design asked Director of Marketing Kory Schroeder if users needed to observe positioning tolerances or layout precautions to preserve the current-sense resistors' accuracy. He responded:

Accurately measuring high currents using current sensing resistors can be challenging. Normally, high currents imply low resistance values to maintain efficiency. With these low resistance values comes the potential for voltage monitoring errors due to the effects of temperature. High currents also inherently translate to higher operating temperatures because of high-power loading and because the sensing circuit is typically in close proximity to the power devices it monitors.

For applications less sensitive to temperature, it is usually sufficient to have high current traces going into the termination ends with sense leads running under the part connected inside of the terminations. However, this method is not adequate for resistance values below 3 mΩ or when the application requires a TCR less than 100 ppm/°C. For those applications, a four-terminal Kelvin connection can greatly improve the sensing accuracy, even if the resistor itself has only single terminations on each side (Figure 1). The solder pad layout that the figure depicts can improve the sensing accuracy by 20% to 50% over single pad layout designs.

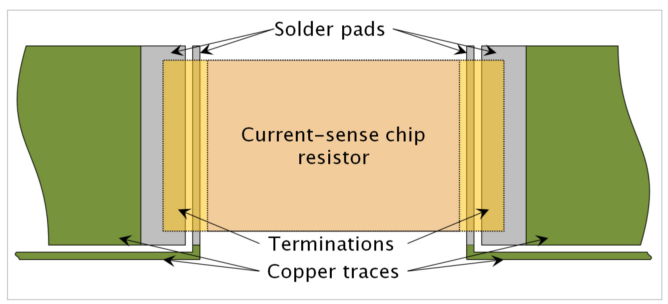

Figure 1: A four-terminal Kelvin connection can greatly improve the sensing accuracy, even if the resistor itself has only single terminations on each side. (Drawing not to scale.)

This design minimizes the effects of termination resistance and TCR by taking the voltage measurement as close as possible to the active area of the resistance element. The large current carrying traces have significantly less thermal influence on the separate sense leads running under the part. This type of layout has proven to be the most useful for high-current applications with demanding requirements for sensing accuracy.

Kory Schroeder, Director of Marketing, Stackpole Electronics

www.seielect.com

POWER ICS DRIVING FORWARD IN AUTOMOTIVE ELECTRONICS

By: Ben Scott

Power-management and IC-driver products are becoming increasingly important as electronic content per vehicle rises.

Moreover, the power-IC market is a lucrative one with a value of $1 billion in 2011, growing to $1.4 billion by 2018, says IMS Research. This opens up many opportunities for the suppliers in this market like Infineon, Maxim Integrated Products and Fairchild Semiconductor.

A large proportion of this value comes from powertrain applications. Power ICs are essential for engine-management systems in petrol, diesel, hybrid, and electric vehicle applications. The market for power ICs in the hybrid and electric space will reach over $50 million this year, but the largest market will be for power discretes and modules. The vehicle's inverter requires power electronics to drive the motor/generator. Alternators and fuel pumps make significant use of power ICs. Automatic transmission control units also make use of power ICs to drive the large number of MOSFETs found in this application. Steering systems use either a brushed or brushless DC motor and there are a number of MOSFETs here which require a power IC.

Stepper motors will become more prevalent in auto-leveling headlight control where a stepper-driver IC will be used. HVAC systems have historically used unipolar stepper motors, but there is a trend towards bipolar stepper motors because of increased efficiency and better torque. Bipolar steppers are more expensive, but are approaching parity with unipolar steppers. Bipolar steppers will use similar driver ICs to those found in headlight leveling.

The high growth expected in this market is also driven from regional legislation on ESC (Electronic Stability Control). In the USA there is legislation that all 2012 model passenger vehicles will have ESC fitted as standard. There is similar legislation in the UK, Canada, and Australia. Clearly, mandatory fitment of this system will drive the power-IC market value upwards. However, in these regions the market for this system will be saturated and the market will stagnate as power IC prices come down.

There is a trend in passenger vehicles for the use of LEDs for front and rear lights, ambient cabin lightning, and backlighting for infotainment and instrument clusters. These are all growth areas for the power-IC market as the LEDs need a driver. The number of LEDs per system will decrease as LEDs become brighter, but the number of power ICs to drive these LEDs will remain roughly the same.

Ben Scott
Analyst, IMS Research

www.imsresearch.com

AUDIOSUSCEPTIBILITY MEASUREMENTS AND LOOP GAINS

By: Dr. Ray Ridley

In this series of articles, Dr. Ridley discusses the four important frequency-response measurements to be made during full characterization of a switching power supply. The important relationships between loop gain and audiosusceptibility measurements are highlighted in this second article. As with output-impedance measurements, it is possible to extract a calculated loop gain from the audiosusceptibility measurements, but direct loop gain is recommended to guarantee rugged stability.

Power Supply Transfer Function Measurements

There are four fundamental transfer functions that characterize the small-signal performance of a switching power supply. They are as follows:

1. Loop gain and phase – determines the stability of your design, and available margin to accommodate variations in components.
2. Output impedance – determines the output regulation, dynamic load response, and susceptibility to complex loading.
3. Audiosusceptibility – determines the transmission of noise from input to output.
4. Input impedance – determines the sensitivity of the power system to input filter or input power system components.

The first two parameters, loop gain and output impedance, were discussed in the first article of this series. It is highly recommended that both of these measurements are made on every switching power supply that you design and build. The loop measurement is essential to guarantee stability over the lifetime of the power supply, and the output impedance gives comprehensive information about the performance in the presence of load variations.

An audiosusceptibility measurement gives information about the transmission of noise from the input of the power supply through to the output. It is usually a requirement of the documentation package in the aerospace industry. This measurement is more difficult to make than output impedance since a perturbation must be injected on top of the high-power input rail. Most commercial designs

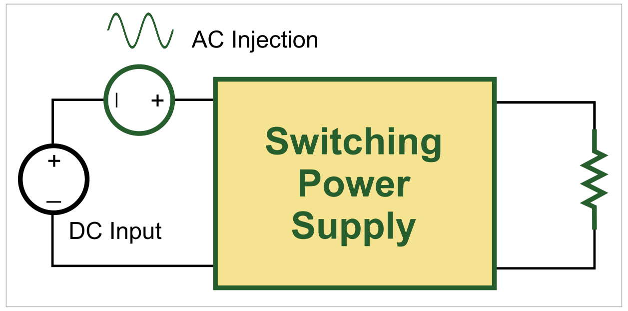

Fig. 1: Audiosusceptibility is measured by adding a voltage signal at the input terminals of a power supply.

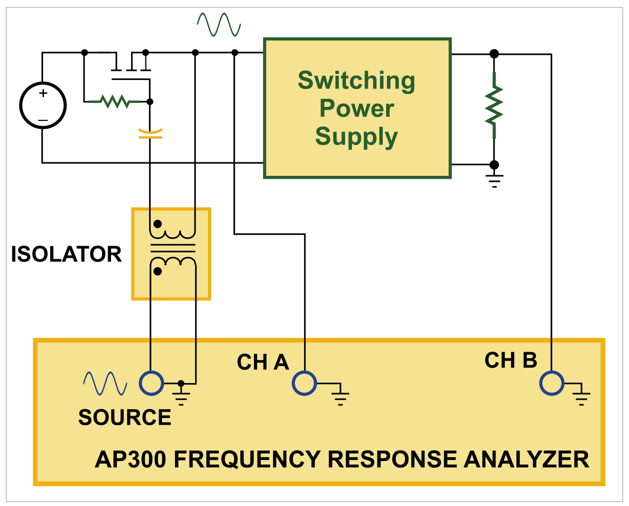

Fig. 2: Practical test setup for injecting voltage signal and measuring audiosusceptibility.

omit this measurement, although it can be very useful for getting maximum performance out of your power supply. With the injection techniques recommended in this article, it is not that hard to make the measurement and it is usually well worth the time.

Audiosusceptibility Measurements

Audiosusceptibility directly shows how well a converter rejects noise appearing on the input. In order to measure audiosusceptibility, a voltage source must be injected in series with the input of the power supply as shown in Figure 1.

Figure 2 shows how this is implemented practically using a frequency response analyzer and a few discrete devices. The output of the analyzer is connected to wide-bandwidth isolator which is then AC coupled to a FET hooked up as a voltage follower. The size and rating of the FET may vary according to the power level and voltage level of the converter that is being driven. This injection technique is much simpler and more cost effective than inserting a high-power amplifier in series with the input source, and will allow sufficient signal to be injected for most applications.

It is useful to plot both the open-loop and closed-loop audiosusceptibility to show how well your control design is implemented. These two measurements are shown in Figure 3 for a sample flyback converter operating with voltage-mode control.

The green curve of Fig. 3 shows the open-loop audiosusceptibility of the converter. At low frequencies, the dc value is determined by the dc gain of the converter and the transformer turns ratio. Above 1 kHz, beyond the resonant frequency, the measured audiosusceptibility is attenuated according to the LC filter characteristics. It is often difficult to make measurements at higher frequencies due to noise pickup in the cables and the small size of the output signal, as indicated by the results of Fig.3.

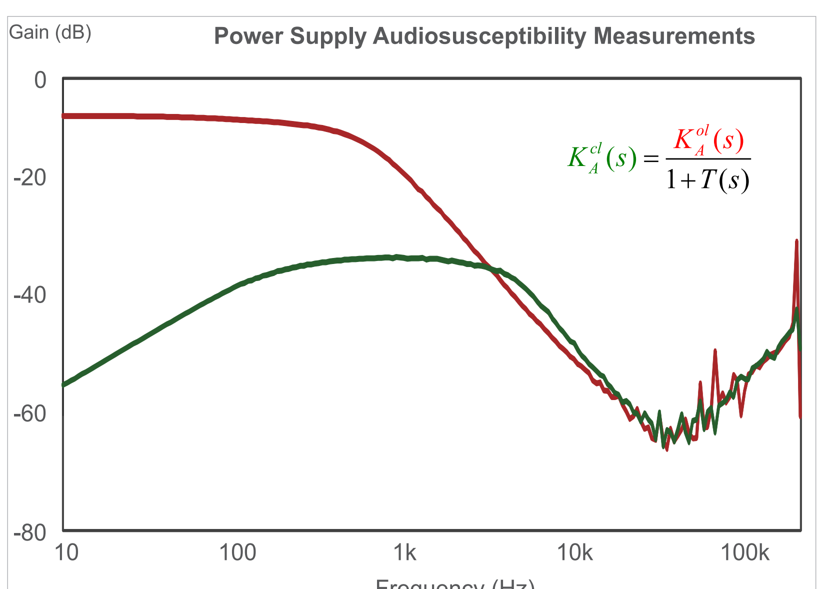

Fig. 3: Open-loop and closed-loop audiosusceptibility measurements of a flyback converter.

The red curve of Fig. 3 shows the effect of closing the loop on the output impedance. At low frequencies, where the loop gain is high, the audiosusceptibility is greatly reduced. The two curves converge together at the crossover frequency of the loop. As is well known for a single-loop feedback system, the theoretical closed-loop audiosusceptibility is related to the open-loop audiosusceptibility by the equation:

$$K_A^{cl}(s) = \frac{K_A^{ol}(s)}{1+T(s)}$$

From this equation we can see that the higher the loop gain T(s), the more the audiosusceptibility is reduced by the feedback loop. When you are designing a power supply, there are two ways to reduce the audiosusceptibility. The first is by increasing the amount of capacitance on the output of the power supply to lower the open-loop audiosusceptibility. This, of course, requires more expense in terms of parts and space. Or, you can increase the gain of the loop. Changing loop components is usually a zero-cost option, but you must be careful not to increase the loop gain too high or instability can result. Some modern converters have very low loop gains and crossover frequencies, resulting in non-optimal performance.

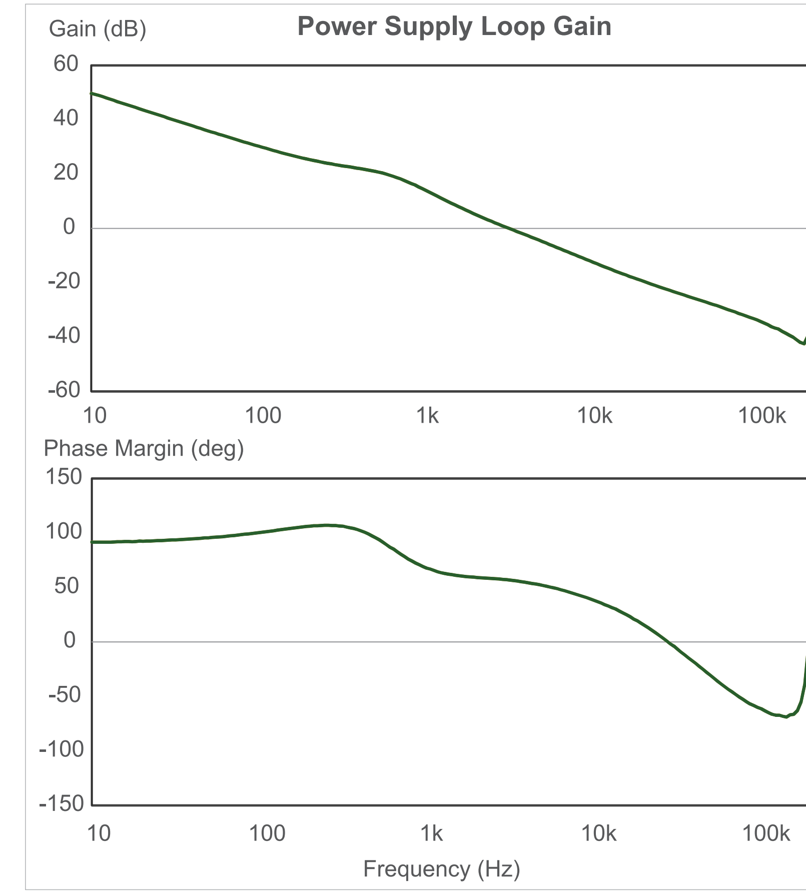

Fig. 4: Measurement technique for loop gain.

Loop Gain Measurements

You should always measure the loop gain of your converter to ensure you are maximizing the performance in terms of audiosusceptibility and output impedance, whilst retaining rugged stability. Fig. 4 shows the test setup for injecting into the feedback loop for accurate results. This setup requires the insertion of a test resistor into the feedback loop, but this is not a difficult process. Further details of using this test setup are covered in detail in [1, 2].

Fig. 5 shows the measured loop results for the flyback converter. The gain at 10 Hz is approximately 50 dB, and this corresponds to the difference in magnitude of the open- and closed-loop audiosusceptibility shown in Fig. 3.

The crossover frequency is at around 3 kHz, and the phase margin at crossover is 60 degrees. The open and

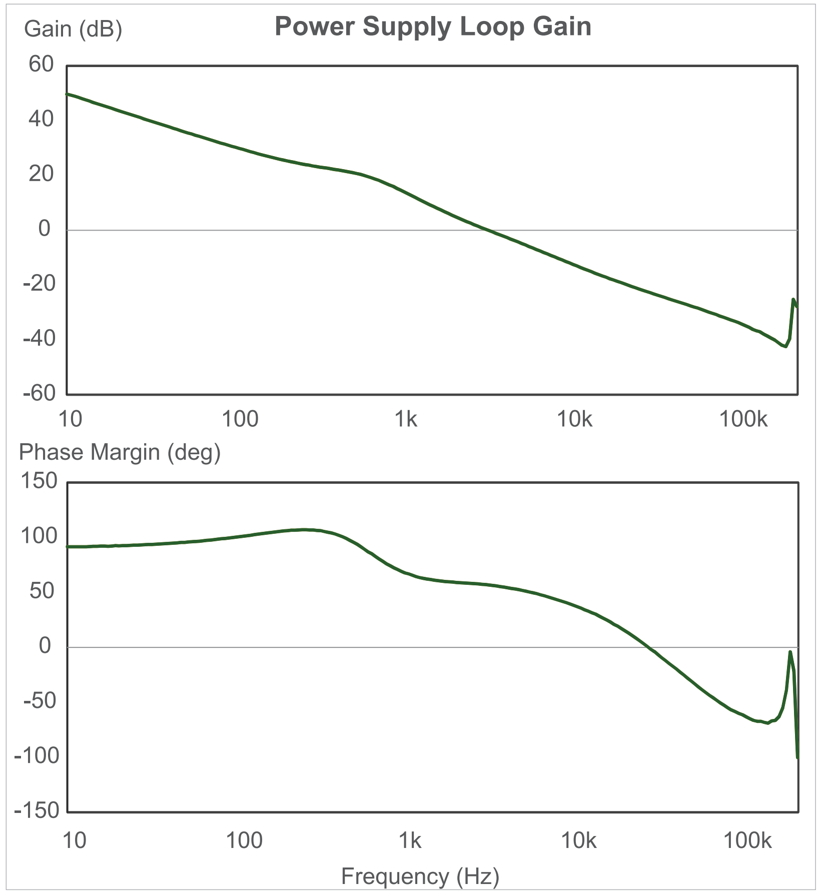

Fig. 5: Direct loop gain measurement of flyback converter.

closed-loop audiosusceptibility measurements are approximately equal at this point. It is interesting to see that beyond this frequency, the closed-loop audiosusceptibility is actually higher than the open-loop measurement. This is because the vector sum of 1+T(s) is less than one as the phase margin of the measured loop drops below 60 degrees. The same effect was observed for the output impedance measurement in the previous part of this series.

Synthesized Loop Gain Measurements

Three measurements have been made so far for this converter – open-loop audiosusceptibility, closed-loop audiosusceptibility, and loop gain. In theory, only two of these measurements should be necessary since the three quantities are related to each other by Eq. 1. In practice, however, we always measure all three quantities since direct measurement of each gives the most dependable results. If we rearrange Eq. 1, we can express the loop gain of the converter in terms of the audiosusceptibility measurements as follows:

$$T(s) = \frac{K_A^{ol}(s)}{K_o^{cl}(s)} - 1$$

From this, we can try to plot the loop gain from just the audiosusceptibility measurements. Note that it is crucial that both the magnitude and phase of the audiosusceptibility measured in order to perform this calculation, even though we commonly only present the magnitude as part of a power supply characterization. Fig. 6 shows the result of this equation plotted against the directly-measured loop. The green curve of Fig. 6 shows the directly-measured loop gain, and the blue curve shows the calculated loop gain, synthesized from the impedance measurements.

Fig. 6: Direct loop gain measurement compared with synthesized loop from audiosusceptibility measurements.

For this power supply example, the measured and calculated loop gains agree fairly well up to the region of the crossover frequency. At high frequencies there is very significant deviation of the directly-measured true loop gain and the gain synthesized from the audiosusceptibility measurements. This is due to the noise pickup in the audiosusceptibility measurements as the attenuation is large. The synthesized loop gain of Fig. 6 is not sufficient to guarantee lifetime stability since gain margin is not measurable, and the possibility of multiple crossings cannot be observed.

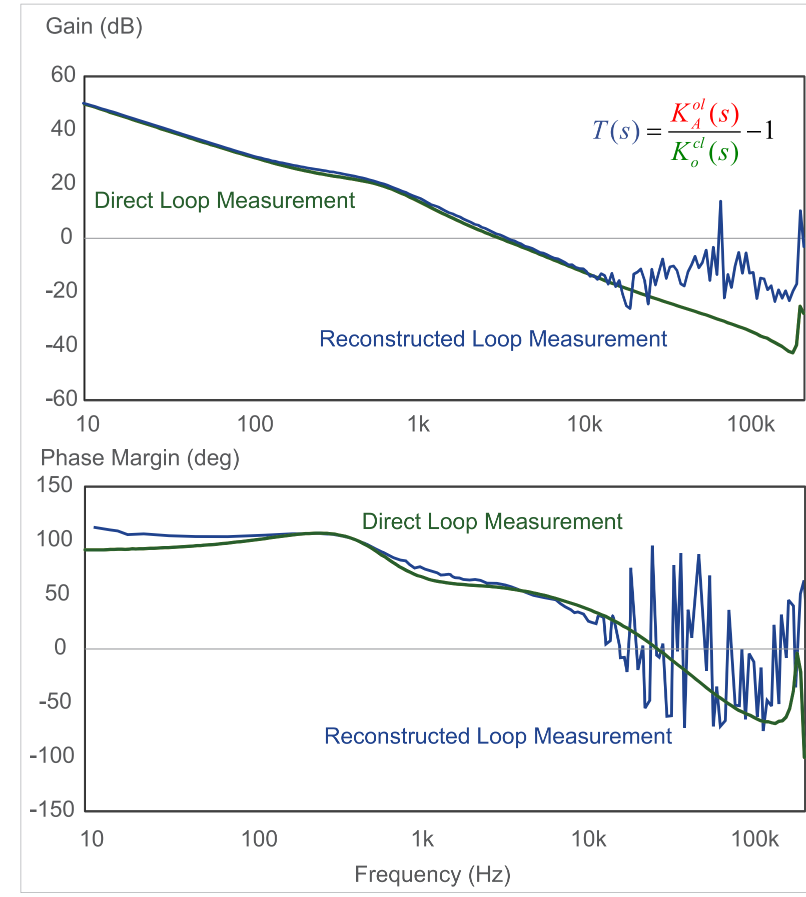

Fig. 6: Direct loop gain measurement compared with synthesized loop from audiosusceptibility measurements.

Summary

This article clearly shows the relationship between loop gain and audiosusceptibility measurements. Most aerospace designs require the audiosusceptibility measurement to be made, but it is also useful for other applications, and it is recommended that you record these measurements as part of a complete documentation package.

In the next article of this series, we will look at the input impedance measurement and its correlation to loop gain.

References

1. Ridley Engineering Frequency Response Analyzer from AP Instruments, www.ridleyengineering.com/index.php/analyzer.html
2. Ridley Engineering Design Center, www.ridleyengineering.com/index.php/design-center.html

Dr. Ray Ridley
President, Ridley Engineering

www.ridleyengineering.com

IMPROVING ELECTRIC-MOTOR TESTING TECHNIQUES

By combining FEA with FPGA hardware, simulation models can include nonlinearties for accurate motor representation

By: Nick Keel and Frank Heidemann

The growing adoption of electric motors in the automotive industry creates new challenges for embedded-control-system developers and test engineers.

Control algorithms for electric-drive ECUs (electronic control units) must run much faster than power-train ECUs for internal-combustion engines. These higher speeds make the traditional approach to HIL (hardware-in-the-loop) testing inadequate for testing electric motor ECUs. Engineers must simulate electric motors with high fidelity, and HIL test systems must be able to execute simulation models at rates on the order of 1 µs to adequately represent the electric motor's operation (Figure 1).

Power electronics introduce another challenge when developing and testing electric-motor control systems. To test the power electronics, the test system must handle voltages that range from 20 to 600 V and current that could be in excess of 500 A.

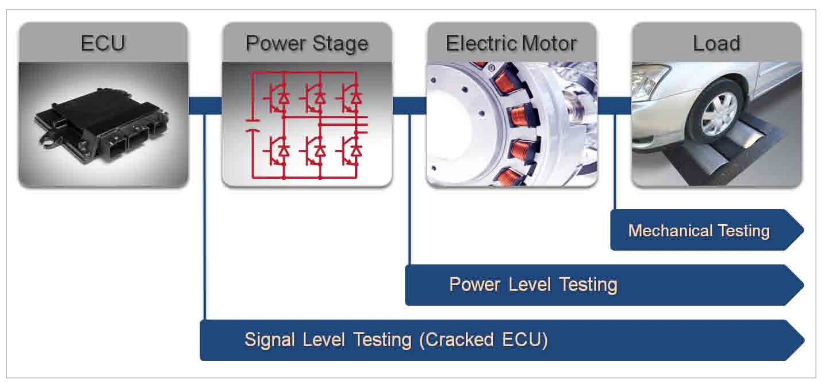

Figure 1: Each stage of embedded-software validation for electric-motor simulation introduces new challenges for test engineers such as high-speed processing and high-power signals.

These types of tests often implement on a dynamometer, but dynamometers are limited in the test coverage that they can provide. They often fail to represent accurately vehicle dynamics, which increases the number of field tests necessary to validate fully an electric vehicle power train. A test system capable of handling high-power signals while accurately simulating vehicle dynamics reduces the number of dynamometer and field tests, and reduces the overall time and cost to test.

Motor simulation using FEA

One of the greatest challenges engineers face when conducting real-time simulation of advanced motor drives is how to attain an adequate combination of model fidelity and simulation step time. While a simple constant parameter D-Q model may be sufficient to conduct some HIL tests, increased model fidelity is often necessary for the design of advanced motor drives.

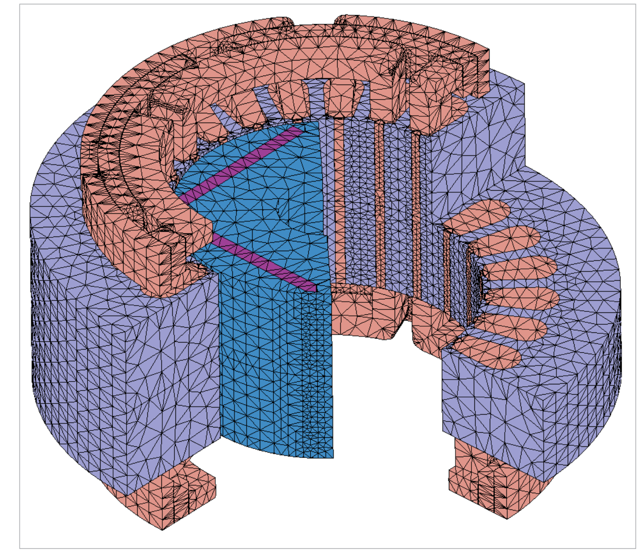

Figure 2: The high density mesh of the FEA (finite element analysis) produces a very high fidelity representation of this IPM (interior permanent-magnet) motor's characteristics.

High-fidelity simulation also applies to performance optimization of control systems in high-efficiency electric motor applications commonly found in the automotive industry. Using high-fidelity FEA (finite-element analysis) models, an engineer can simulate complex, non-ideal behavior such as cogging torque and design a controller to reduce torque ripple.

Similarly, a designer can simulate the variation in motor inductance at high currents, which greatly affects the torque produced by the motor, and test the controller accordingly. Lower-fidelity models do not adequately represent cogging torque, motor inductances at high currents, or other nonlinearities in the simulation. The absence of these characteristics reduces the effectiveness of HIL testing, which results in more field tests and increased development time to test adequately embedded-control software.

FEA is a simulation method that provides highly accurate motor models with enough fidelity to account for nonlinearities found in electric motors (Figure 2). However, historically, this high fidelity simulation has been limited to software-only implementation, because it can often take hours to simulate a few seconds worth of real-world operation.

To perform HIL testing on electric motor systems, simulation models must run in real-time. High-fidelity models need simplifying to run within the limits of processor-based systems, resulting in reduced effectiveness of HIL tests. A processor-independent, hardware-based simulation is necessary to achieve the closed-loop update rates required for electric-motor HIL testing.

FPGAs provide the high speed processing necessary for electric-motor simulation and high-speed update rates with low latency from input to output. However, because FPGAs are hardware, they have limited available resources.

Engineers must often simplify electric-motor models to operate within the limits of these resources, which reduces model fidelity. To obtain the performance and accuracy necessary for real-time high-fidelity electric-motor simulation, an FPGA must be large enough to contain the entire characterization of the electric motor.

Advancements in FPGA technology have made it possible for tools such as the JMAG add-on for NI VeriStand to perform real-time high-fidelity simulation of electric motors for HIL testing. Meanwhile graphical-programming tools such as LabVIEW FPGA provide an abstracted tool chain for FPGA development that reduces development time for creating high-fidelity electric-motor models.

High-power HIL testing

While signal-level testing provides much value for developing control algorithms and evaluating ECU performance, it is important

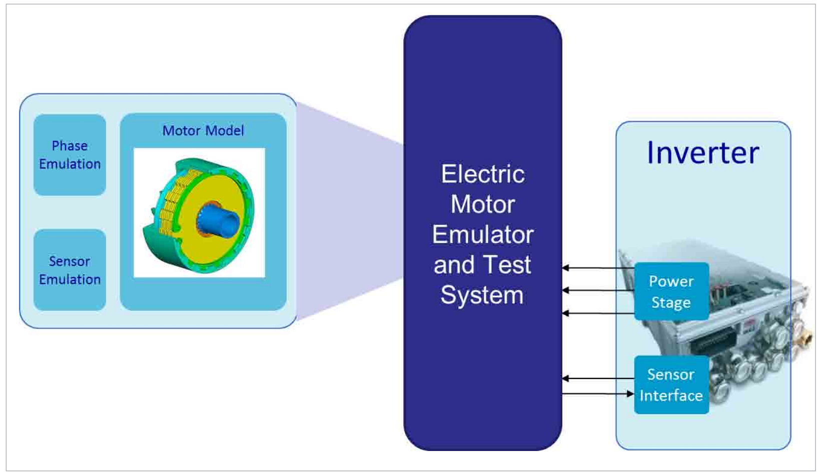

Figure 3: In an electric-motor emulator test system, the emulator inputs the high-power signals from the power stage and closely represents the dynamics of the system's missing components.

to also validate the power electronics associated with the system. Dynamometers are common for power-level testing, but they cannot accurately represent high-frequency dynamics needed to adequately validate system performance.

The lack of test coverage dynamometer testing achieves forces test engineers to perform extensive field tests, which results in reduced test coverage and higher overall test costs. An HIL test system capable of integrating power electronics and simulating vehicle dynamics provides test coverage not found in dynamometer testing.

In the case of an electric-drive dynamometer, the original electric motor in the drive train couples to another electric motor that the test system controls. This electric-motor-dynamometer configuration involves an electric drive tested together with a controller that includes high-voltage power electronics.

The problem with this procedure is that the rotating test system itself constitutes a drive train with drive shafts and load machine, but it has nothing in common with the vehicle into which the electric motor will eventually operate. This renders it almost impossible to model mechanical feedback and turning-speed dynamics from the vehicle with any level of accuracy.

This is a serious disadvantage since electric-motor speed does not always couple to vehicle speed, especially in hybrid drives. In many real-world scenarios, there are intermediate states with gears disengaged and no drive to the wheels, which leaves the electric motor to turn without any load.

The test system cannot reproduce the resulting turning speed dynamics in the rotating test system, because the inert masses involved are too different from those in the future vehicle. This forces engineers to test the ECU in a test vehicle on the road.

An inverter test system, or electric-motor emulator, bridges this gap between the HIL test system and vehicle field tests (Figure 3). This system can interact with high-power signals associated with inverters, and it allows engineers to reproduce load and ambient conditions in the lab exactly as they occur in a drive inverter under field conditions. System level testing that accurately simulates real-world conditions helps test engineers find faults earlier in the embedded software development process, which reduces costs and minimizes development cycles while yielding test data of higher quality.

In practice

Real-time high fidelity electric motor simulation makes it possible to test many types of transient and fault conditions that would be difficult or impractical to perform with the real systems. In the past, many of these conditions such as faults on motor terminals or faults between DC and AC busses have been impossible to implement during HIL testing with standard DQ electric-motor models.

By combining high-fidelity FEA with high performance FPGA hardware, simulation models can include complex non-linear behavior for accurate motor representation. The signals from the model running in FPGA can then connect to other hardware at the high I/O rates necessary for complete testing.

Electric-motor emulators are useful at very early stages in developing and testing hybrid drives and other drives with electric motors. Engineers can map any electric motor type using an integrated emulator, which will behave like the corresponding physical motor in dynamic turning-speed operation.

Emulators also allow developers to model phenomena not yet accounted for in controllers such as harmonic vibrations in electric motors and cancelling out acoustic effects in control engineering. The system runs like a physical motor, but without any moving parts. This means that engineers can run a wider range of tests and collect more accurate data, which reduces time spent with field tests and produces better embedded software.

Nick Keel
Product Manager, NI VeriStand
National Instruments

Frank Heidemann
CEO
SET GmbH

www.ni.com

www.setgmbh.com

REDUCE STAND-BY POWER LOSS IN AC—DC SUPPLIES

New digital power controllers satisfy strict stand-by dissipation standards for consumer-electronics.

By: Scott Brown

Over the past decade, controller-IC manufacturers have worked to reduce so-called vampire or stand-by power consumption.

Organizations such as Energy Star in the US, Blue Angel in Germany, and CNIS (China National Institute of Standardization) have introduced strict stand-by power-consumption standards for consumer electronics. New topologies in the AC—DC power-supply market need implementation to achieve the approvals of these important standards agencies. Traditional flyback converters designed with legacy analog controllers can struggle to achieve the combination of low cost, high operating efficiency, and low stand-by power consumption that today's consumer electronics require. The market now demands new topologies that address all AC—DC feature and performance requirements at low BOM cost.

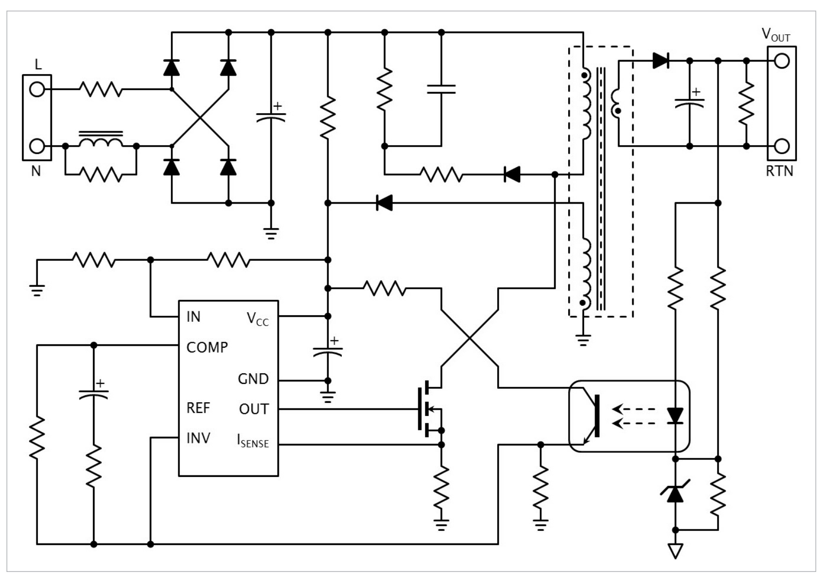

Figure 1: A simplified diagram of a typical 10—20 W flyback converter for isolated off-line applications.

With the typical number of small appliances and electronic devices in an average household rising to 24 over the past decade, the consumer electronics and home appliances market reached its zenith despite one of the largest global economic downturns in a century (Reference 1). With the number of powered devices in our homes increasing, the demand on the electrical power grid is expanding at an equivalent rate. Many governments, realizing the economic and environmental ramifications of the ever-increasing electrical load have implemented strict energy standards to limit the power consumption of these electronic devices while they're operating and, more importantly, while they're in stand-by mode.

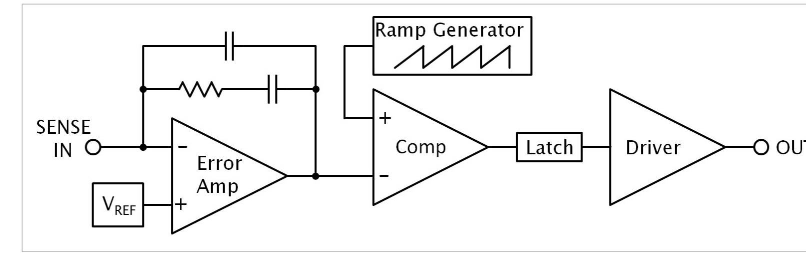

Figure 2a: An analog controller directly monitors the converter's output voltage.

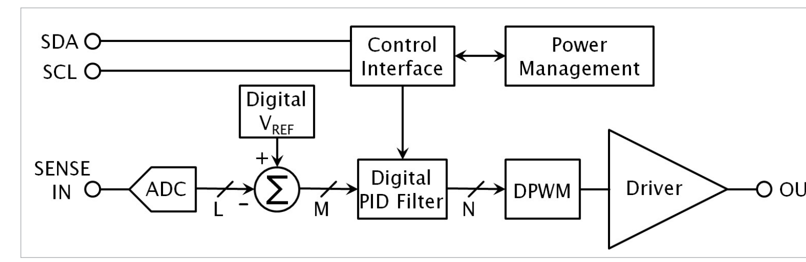

Figure 2b: A digital converter can switch operating modes without complex compensation schemes.

The biggest problem area is the main power supply, whether for powering plugged-in electronics or the charger for portable electronics. Traditional approaches use power supply technologies that waste energy at low output power as a consequence of keeping costs down. The industry needs new techniques to reduce power consumption when the load is virtually zero without increasing system cost.

Traditional analog PWM ICs

The main off-line AC—DC power supply for consumer electronics traditionally uses a simple analog PWM (pulse-width modulation) controller IC and low-cost external components. To keep cost to a minimum, the designer generally uses a generic analog PWM controller, typically a controller that could apply to multiple configurations with a minimum of internal complexity. With these basic controllers, the main power-supply topologies are typically isolated flyback or forward converters, requiring a large number of external components and output feedback from a costly opto-isolator and several discrete components for external frequency compensation (Figure 1).

Most of these analog controllers are simple PWM controllers which operate in full PWM mode regardless of the load conditions. This works well at full output power, but efficiency, η, quickly degrades at medium and light loads, making it difficult for these legacy controllers to meet modern efficiency requirements, which use an average η calculation based on output power to set a minimum η requirement. At light load currents, the legacy controllers will have efficiencies well below 70% that pull down the average, making it difficult for these converters to meet the new standards. Designers can implement additional modes of operation, such as PFM (pulse-frequency modulation) or pulse-skipping to improve η, but this adds complexity and circuit cost that may be burdensome for the mainstream market.

Digital control technology for power supplies has been around for several years but it has now matured to the point where the cost—performance tradeoff can better that of analog alternatives. In the case of off-line power supplies, digital control blocks' benefits surpass those of analog-equivalent blocks.

Domain makes a difference

The analog block monitors

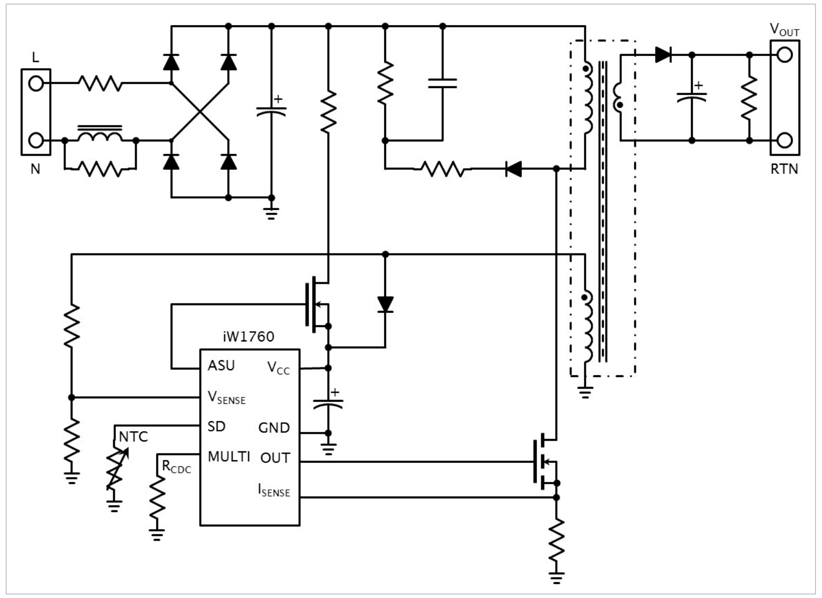

Figure 3: A flyback converter implemented with a multi-mode digital controller maintains high η over a large current range.

voltage directly and modulates the output based on that input (Figure 2a). In contrast, the digital block converts the traditional analog input into a digital signal, which it then filters and processes to determine the output conditions (Figure 2b). The digital converter, however, achieves a degree of freedom that the analog circuits cannot: The digital block can quickly modify the modulation scheme, matching the converter's operating mode to the system's needs, increasing η without sacrificing performance. Additionally, because digital algorithms manage the loop compensation, there is no concern about stability and, in some cases, no need for external compensation components. In the event of heavy loads, the controller can drive the output at its highest programmed switching frequency to maximize η. When the load current falls to a level where the switching losses become an important efficiency factor, the digital controller can change the modulation from PWM to PFM, reducing the average switching frequency and saving power. Digital control makes it possible to implement this type of dynamic multi-mode approach cost-effectively.

Multi-mode increases η

For example, iWatt's iW1760 is a digital controller that integrates a multi-mode digital modulator to increase efficiency. The circuit example (Figure 3) and the typical operating curve of (Figure 4) illustrate the power of digital control technology: The device offers four distinct operating modes, PWM, PFM, DPWM (Deep PWM) and DPFM (Deep PFM) to maintain a high average η.

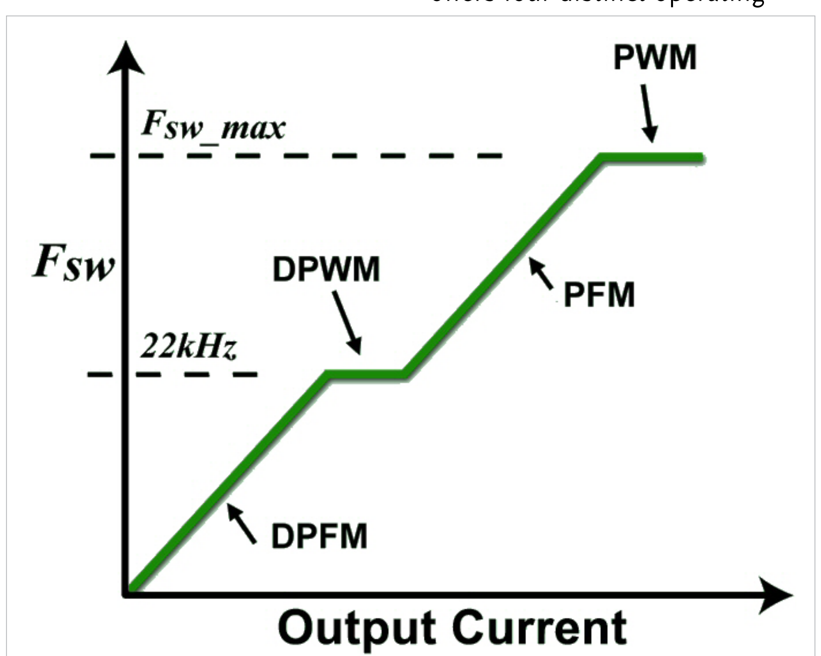

Figure 4: Multi-mode operation—switching frequency as a function of load current.

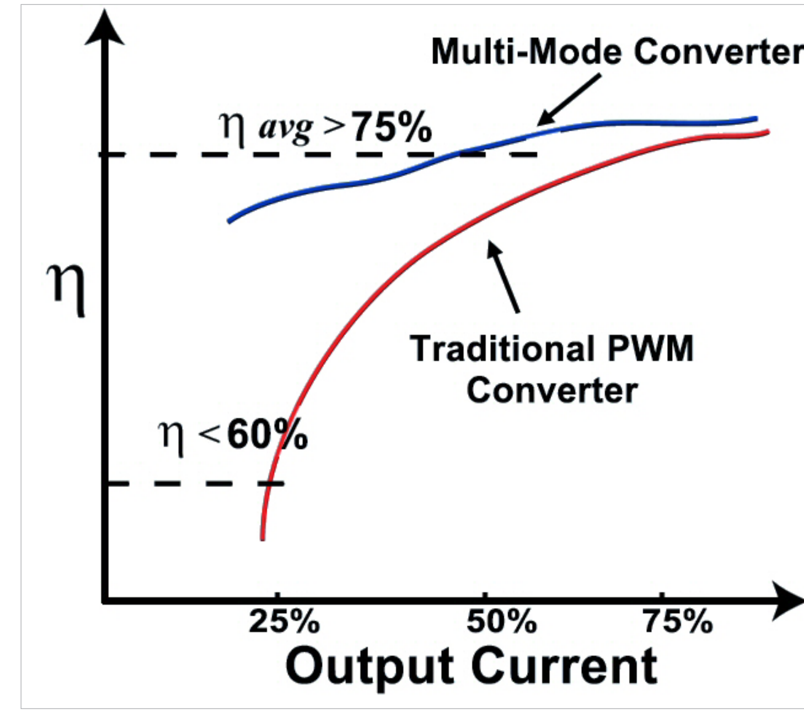

Figure 5: Efficiency comparison between a multi-mode converter and traditional PWM converter implementations.

The converter operates in full PWM mode with a constant frequency at high output currents. When the output current reaches a calculated minimum threshold, the converter switches to PFM mode, increasing the off time to save energy.

As the load current decreases to the point where the PFM switching frequency would possibly enter into the audible spectrum (no less than 22 kHz), the device automatically switches into DPWM mode, holding the switching frequency constant at 22 kHz. When the load current drops low enough, the digital block changes the converter into DPFM mode, where the switching frequency drops into the audible range, but at power levels so low that the converter does not emit audible noise.

An analog controller, operating in full PWM mode at very light loads will end up dissipating 0.5—1 W just in power lost in the external components and the operating current of the controller itself. This power consumption is beyond the levels that standards organizations such as Energy Star have established (Figure 5).

By using the digital control block, the user enjoys efficiency levels greater than 80% at full load and an average efficiency over a broad operating current range greater than 75%. Modern digital controllers, such as the iW1760, can achieve a no-load power consumption of only 50 mW. This is well below Energy Star's requirement that AC—DC external power supplies consume 300 mW or less in stand-by mode.

Fewer components

Besides the efficiency gains, digital control also allows designers to reduce the external component count. By managing compensation in the digital domain, designers can remove several passive components from the schematic.

The digital controller can also implement primary-side control without sacrificing regulation performance. This allows the circuit to provide an isolated output without an opto-isolator, a component that is costly and is one of the weak links in power supply reliability.

Scott Brown
Senior VP of Marketing
iWatt

www.iwatt.com

References:

1. Market Research Report: Trends in CE Reuse, Recycle and Removal, Consumer Electronics Association, March, 2008.

ESTIMATING BOND WIRE CURRENT-CARRYING CAPACITY

Analysis provides insight into bond-wire performance in various configurations for power-management ICs.

By: Jitesh Shah

Semiconductor manufacturers use wire bonds extensively to connect a chip's I/O pads, including power, to its package's external pins.

Wire bonding processes typically use gold wire because of its oxidation resistance, high electrical conductivity, and the relative ease with which it bonds to the IC's pads and the package's pins. An approach involving replacing gold wire with copper is gaining strength due to copper's superior electrical and thermal properties, lower intermetallic growth, and increased mechanical stability.

Devices that pass high DC currents use multiple bond wires. The extra wires reduce the DC IR drop and its associated heating to reduce the risk of wire fusing. Unfortunately, there is no method or analysis in place to estimate the number and size of wires to use for a given application. Either the number of wires used is too pessimistic, increasing the die area and cost, or too optimistic, decreasing the device's reliability.

The theoretical estimate

The classical design equation for wire fusing was developed by W.H. Preece in 1884 and applies only to wires in free air. The Preece equation relates the fusing current in amperes to the diameter of the wire in inches:

WIRE DIAMETER	PREECE EQUATION	MODIFIED PREECE EQUATION (MIL-M-38510J)	
(Mils)		Conductor Length ≤ 0.040"	Conductor Length > 0.040"
2	0.92	2.68	1.83
1.3	0.48	1.41	0.96
1.2	0.43	1.25	0.85
1	0.32	0.95	0.65
0.9	0.28	0.81	0.55
0.8	0.23	0.68	0.46
0.7	0.19	0.56	0.38
0.6	0.15	0.44	0.30

Table 1: Current-carrying capability based on Preece equations

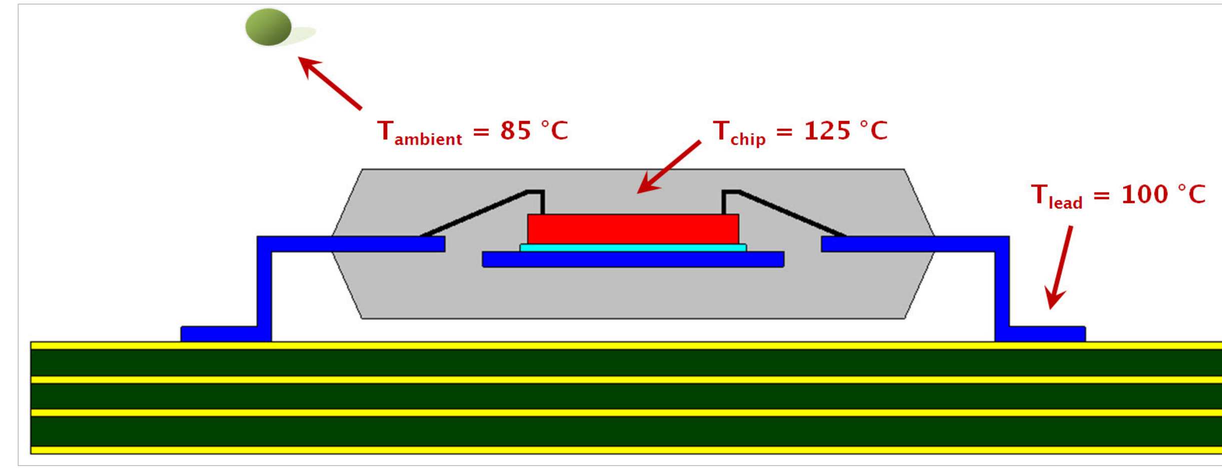

Figure 1: Package on a PCB with relevant temperature-monitor points

$$i = kD^{\frac{3}{2}}$$

where i is the DC or RMS current, k is a constant corresponding to wire composition, and D is the diameter of the wire in inches. For gold and copper, k = 10,244.

One of this equation's limitations is that it applies only to wires in free air. Additionally, it does not consider the fact that the current carrying capability of a wire varies inversely with its length.

Modified Preece equation

One way to address these limitations is to modify the Preece equation with a higher value of k to reflect typical packaging processes that encapsulate the bond wire with an epoxy-based molding compound. The constant k also reflects the effect of length on the wire's current-carrying capability. The value of k for conductor length ≤ 0.040" for both gold and copper is 30,000 and for conductor length > 0.040" is 20,500.

The equation Military specification MIL-M-38510J presents bases its current-carrying capability assessment on the modified Preece equation. Table 1 lists the calculated current-carrying capability in Amperes of both conductor types using the two versions of the Preece equation.

Two limitations remain with the modified Preece equation. It produces current-carrying-capability values that are material-independent. Copper has 20% higher thermal conductivity and 30% higher electrical conductivity than gold, which should result in copper being able to carry more current than gold for a given bond wire length and diameter.

The equation does not extrapolate the current carrying capacity with conductor length beyond 0.040" (about 1 mm). Most applications use wire lengths in the 2- to 3-mm range or longer. A wire's current-carrying capability varies dramatically as conductor length changes, which the equation fails to consider. Given these limitations, a new approach is necessary that accounts for known geometry and material properties and on limitations typical applications impose.

Joule heating in conductors

Current flowing through a non-ideal conductor—one with non-zero electrical resistance—converts electrical energy to thermal energy through a process called Joule heating or resistive heating. The magnitude of heat the processes generates is directly proportional the wire resistance and to the square of the current:

$$Q_{generated} = I^2R$$

For a conductor surrounded by still air, all heat generated dissipates through the conductor with negligible heat conducted

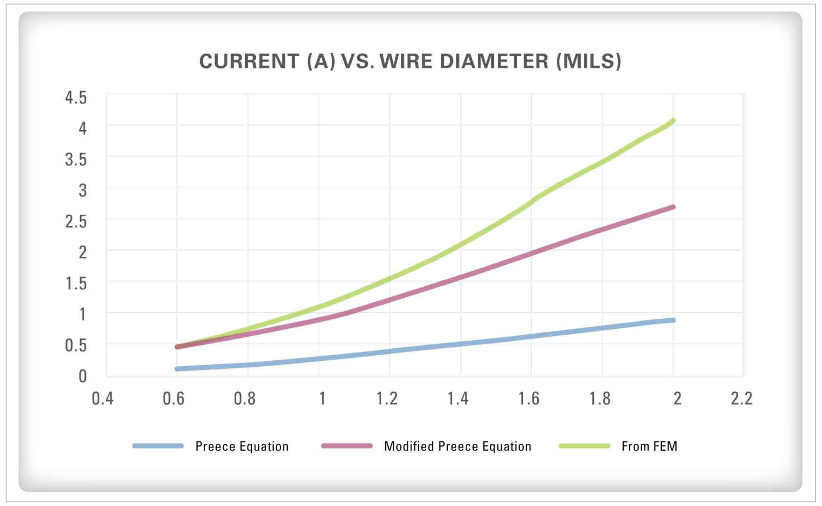

Figure 2: Current-carrying capability of 1-mm-long gold wire using FEM and the Preece equations

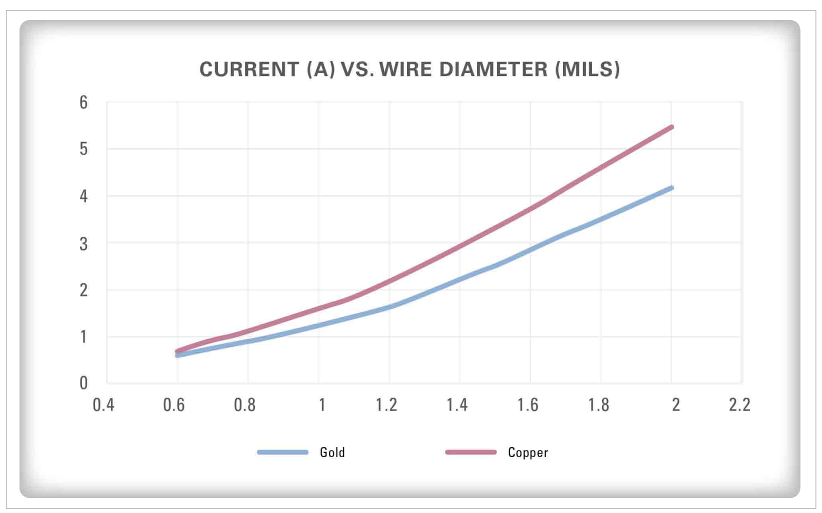

Figure 3: Current-carrying capability of 1-mm-long gold and copper wires using the FEM approach

away from the conductor surface. The system reaches steady state when:

$$Q_{generated} = Q_{dissipated}$$

The generated heat dissipates through the length of the wire using a simple conduction heat-transfer process:

$$Q_{dissipated} = kA\frac{dT}{dx}$$

where k is the wire's thermal conductivity (310 W/mK for gold and 390 W/mK for copper), A is the cross-sectional area of the wire, dT is the temperature differential at the two ends of the wire, and dx is the wire's length.

Rearranging and simplifying,

$$I = \frac{\pi}{4}\sqrt{\frac{k}{\rho}\frac{D^2}{l}}\sqrt{\Delta T}$$

where ρ is the wire's resistivity (2.44x10-8 Ω-m for gold and 1.68x10-8 Ω-m for copper), D is the wire diameter, l is the wire length, and ΔT is the temperature difference between the wire's two ends, which we assume to be a constant for a maximum current-capacity calculation. Simplifying even further,

$$I \alpha \sqrt{\frac{k}{\rho}\frac{D^2}{l}}$$

Based on the above relationship, assuming everything else remains the same, copper should be able to handle 25% more current than gold.

In most practical applications, heat does not just conduct away through the wire but also conducts away in the radial direction from the surface of the wire through the epoxy-molding compound. The combined phenomenon is complex and not subject to analysis with closed-form equations but yields using finite-element modeling software with a thermal-electric-coupled physics solver to examine the effects of different wire parameters.

Model setup

A typical wire-bond process connects the chip's I/O pads to the package's leads with wires, predominantly gold or copper (Figure 1). Manufacturers limit the IC's maximum-ambient operating temperature to 70 °C for commercial applications;

WIRE DIAMETER	GOLD			COPPER		
(Mils)	1mm long	2mm long	3mm long	1mm long	2mm long	3mm long
2	4.075	2.11	1.425	5.45	2.8	1.89
1.3	1.8	0.97	0.665	2.41	1.275	0.87
1.2	1.563	0.847	0.58	2.065	1.1	0.76
1	1.12	0.625	0.435	1.475	0.81	0.56
0.9	0.94	0.525	0.368	1.225	0.677	0.47
0.8	0.76	0.435	0.309	1	0.55	0.394
0.7	0.612	0.355	0.254	0.787	0.45	0.322
0.6	0.475	0.28	0.203	0.608	0.355	0.255

Table 2: Summary of current values in Amperes for different wire combinations

85 °C for industrial uses. Most devices specify a 125 °C maximum chip-junction temperature.

To estimate the bond wires' current-carrying capacity under worst-case conditions, the models assume the industrial ambient temperature with the maximum chip junction temperature. Natural convection boundary conditions apply to the package surface, with the package lead temperature at 100 °C.

A small amount of current through the wire does not change the temperature profile across the span of the wire with the two ends still at the original temperature. As the current increases, the hottest temperature is no longer at the chip junction, but is somewhere in the middle of the wire span.

The glass transition temperature, Tg, of the mold compound is the temperature at which the material transitions from a hard and relatively brittle state to a soft, rubber-like one. A typical Tg is about 150 °C. If the current causes the mold-compound temperature to exceed Tg, time and temperature will degrade the epoxy's chemical bonds at this interface. This not only causes an increase in the thermal resistance of the mold compound, but also results in an increase in the porosity of the material, exposing it to the ingression of moisture and ionic contaminants. A wire-mold-compound interface temperature of 150 °C is, therefore, the upper temperature limit to calculate bond wire current-carrying capability.

With this as the criterion, the effects of wire-material type, wire length, and wire diameter are calculable and a comparison is possible to the theoretical estimates. Figure 2 shows the current-carrying capability of 1-mm-long gold wire using the three approaches. The current value using FEM starts out at about the same level that the modified Preece equation gave but then diverges as the wire diameter increases. The FEM analysis shows the current-carrying capability of gold and copper wires modeling 1-mm-long bond wires (Figure 3) and wires of several lengths (Table 2).

Jitesh Shah
Principal Engineer
Integrated Device Technology

www.idt.com

IMPROVE SET-TOP-BOX SUPPLY EFFICIENCY

Self-timed synchronous rectification resolves timing issues that hamper flyback converters.

By: Yong Ang

With growing urgency to support green initiatives, set-top-box power-supply engineers are reviewing AC-DC topologies to reduce power loss during both active and standby modes.

The flyback converter is one of the topologies that suit offline-conversion power levels from 10 to 60 W, and is the topology of choice due to its low component count and simple control scheme.

Timing issues, however, make it difficult to substitute efficient synchronous rectification for lossy secondary-side diode rectification within a typical flyback converter. However, a self-timing approach overcomes this problem, and helps set-top box power-supply manufacturers achieve efficiency standards that the USA leads with its Energy Star program, and that other world authorities are following.

Active mode efficiency

A universal input AC-DC set-top box power supply typically comprises an input-rectification stage with a storage capacitor, an isolated converter that down converts the high-voltage DC bus as efficiently as possible to the low voltages the various loads require. Of the available isolated converter topologies, the most popular is

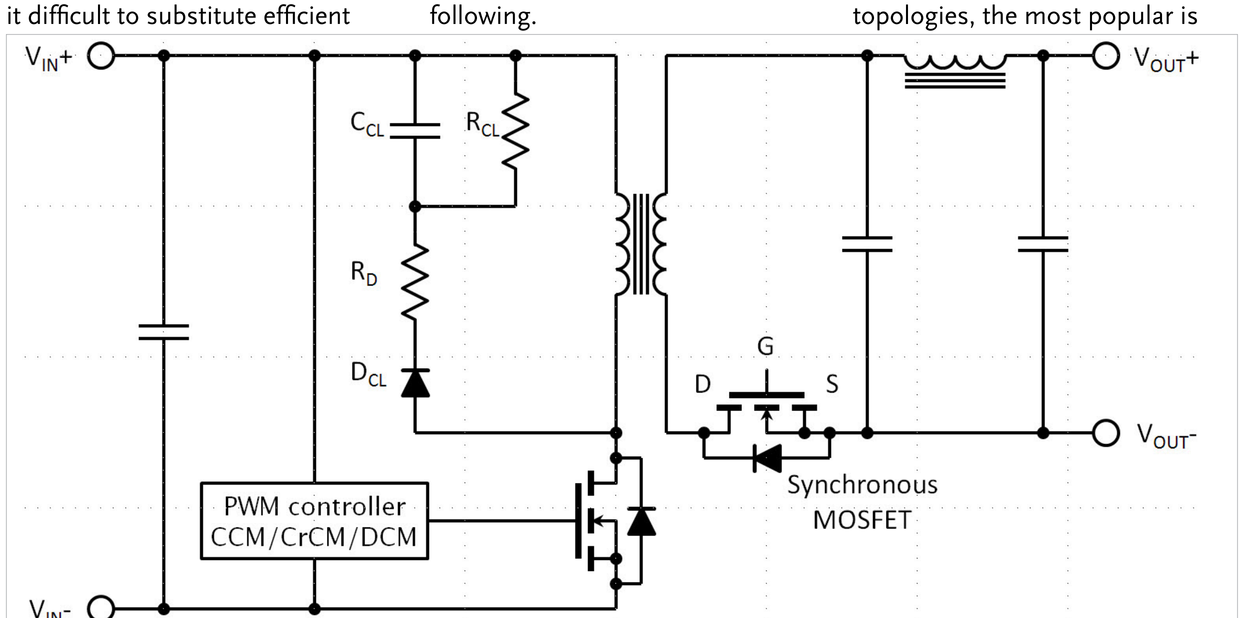

Figure 1: Flyback converter

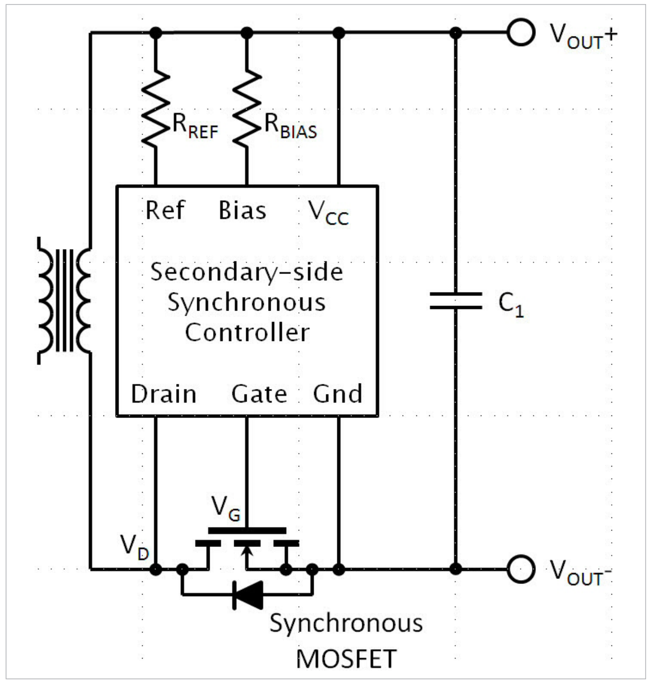

Figure 2: Drain voltage sensing synchronous controller with analogue gate drive for flyback converter.

a flyback converter with multiple transformer secondary windings.

However, increasingly sophisticated set-top-box functionality increases demands on power density and power dissipation in active mode. Designers now have to migrate from multiple- to single-output flyback converters to achieve the necessary performance (Figure 1).

This flyback converter provides a 12 V output. An array of point-of-load converters steps this voltage down to the lower potentials the different internal loads require.

Increasing efficiency

Critically, the output rectifier of a flyback converter is a significant source of conduction-loss, since even the highest performance Schottky diodes will have a relatively high forward voltage when conducting large currents. As a result, secondary-side synchronous rectification has become widely recognized as the way to improve upon the great inefficiency of traditional diode rectification. Precise gate-drive control is essential for synchronous rectification, and three different control schemes are possible.

One scheme synchronises the gate-drive signals for the secondary-side MOSFET rectifier with the primary-side MOSFET's gate drive using pulse transformers. For a flyback topology with multi-mode operation however, this method has difficulty in producing secondary gate-drive signals that are usable over the full load range. This is because the converter operates in a pulse-skipping mode under light load conditions, causing the output rectifier current to become discontinuous and a conduction dead band to exist between primary- and secondary-side currents. The timing mismatch causes reactive power flow between the output and power transformer due to the output capacitor discharging during the discontinuous rectification interval. This causes inefficiencies that effectively restrict the scheme to a narrow load range.

An alternative scheme employs a signal the converter derives from the transformer secondary to drive a synchronous MOSFET. This approach senses the synchronous MOSFET current with a current sense transformer and a high-speed comparator. The signal from the comparator drives the secondary MOSFET through buffer transistors. Although the MOSFET can switch on or off, depending on the state of its current, this method can still suffer from high circuit complexity and comparator timing delay. Lossless drain-voltage sensing overcomes such problems and improves conversion efficiency while reducing system cost by dispensing with the current-sense transformer and comparator (Figure 2).

The self-timed controller

An example of a secondary-side synchronous controller IC, the ZXGD3105, operates closely with the MOSFET that replaces the traditional Schottky diode. The IC senses current by monitoring the forward voltage drop across the parasitic diode within the MOSFET when the diode conducts. When the controller detects diode conduction, it drives the MOSFET gate, turning on the switch after a

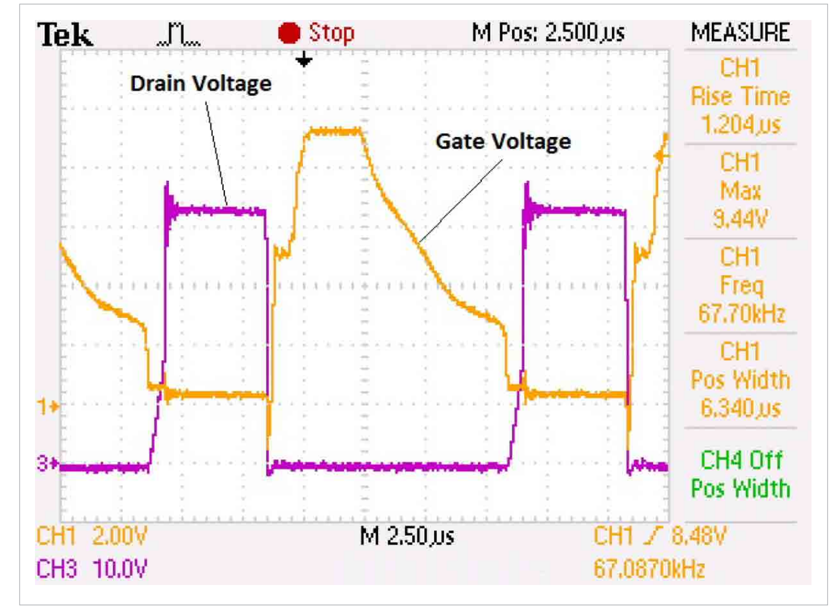

Figure 3: Synchronous rectifier control waveforms in flyback converter at full load.

short 70 ns delay.

At the close of the conduction cycle, efficiency considerations make it imperative to switch the MOSFET off as closely as possible to the zero-current point, preventing the MOSFET from going into reverse conduction. The controller compares the drain voltage to a -10 mV threshold and pulls the MOSFET's gate-drive voltage down, when the drain voltage is more positive than this threshold value. This arrangement switches off the MOSFET at the optimum time.
An interesting feature of the controller's implementation is its use of an analogue signal to control the MOSFET's gate, rather than the digital high voltage that traditional gate drivers use to enhance the MOSFET throughout its conduction period. The gate-drive voltage is proportional to the sensed voltage. The MOSFET controller features an ultra-low quiescent current—1.05 mA, typical—which ensures low no-load power consumption, critical for set top boxes, which spend most of their time in standby mode.

Figure 3 shows the controller quickly ramping up gate voltage as drain current level reaches its peak, fully enhancing the MOSFET to minimise its on-resistance, while it carries significant current. The voltage drive to the MOSFET gate reduces as the transformer flyback current decreases through the MOSFET. This adaptive reduction in gate-drive voltage reduces gate charge in the MOSFET, minimising switching power losses, while speeding the device's turn-off to prevent reverse current flow. The proportional gate driver supplies gate voltage to the MOSFET until the drain current is close to zero, minimising parasitic diode conduction time after the MOSFET switches off.

		Schottky Diodes	ZXGD3105 13 mΩ MOSFET	Percentage loading
Input power	mW	91	141	No-load
Efficiency	%	82.5	84.3	25%
Efficiency	%	84.1	85.7	100%

Table 1: Standby and active mode efficiency in a 30W flyback power supply at 230Vac.

Tests assessed the extent to which a dedicated MOSFET gate controller delivers power savings in a set-top-box flyback power supply's output-rectification stage configured for a universal AC input and a 12 VDC, 30 W output. Table 1 compares the performance of the controller with that of a traditional Schottky-based design in terms of power loss and efficiency.

The test result demonstrates that synchronous rectification using a MOSFET controller can achieve a 1.6% efficiency improvement at full load over a Schottky design, while ensuring the power-supply standby power is within the 300 mW Energy Star limit.

Yong Ang
Applications and Technical Marketing Manager
Diodes Incorporated

www.diodes.com

Special Report:
Automotive

PSD NORTH AMERICA
Power Systems Design: Empowering Global Innovation

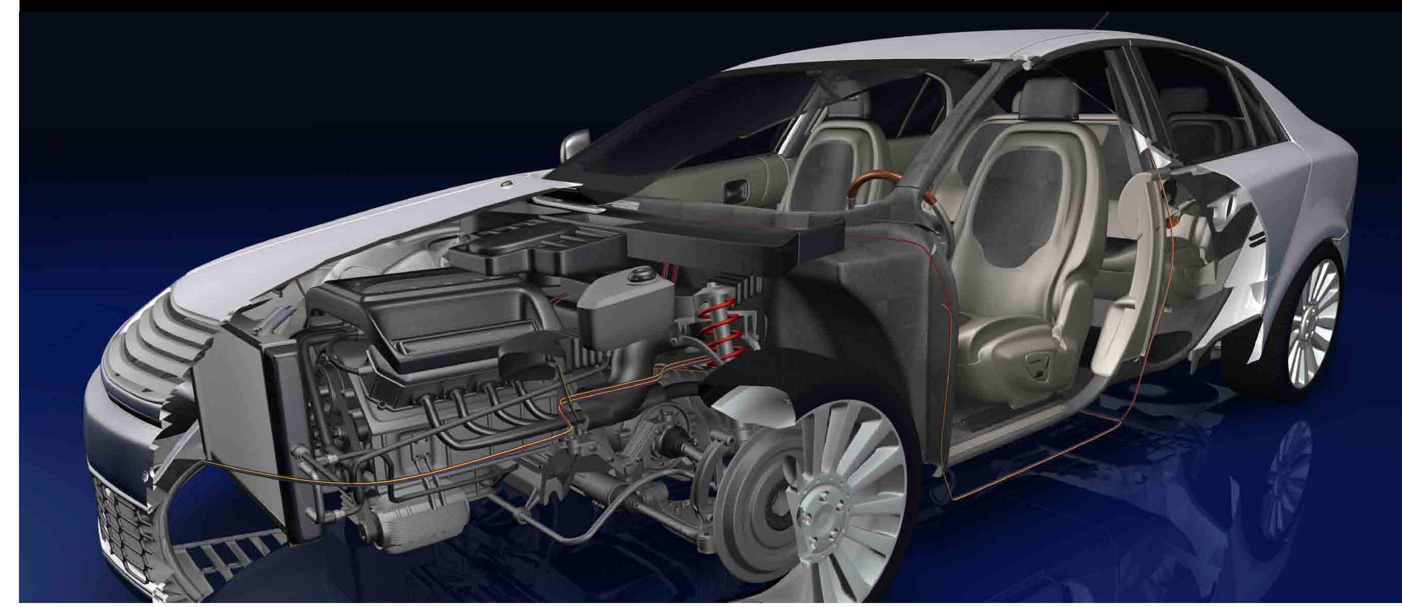

Inside:

Sleeping Conserves Energy... 32
Hall-Effect Current Sensing in HEVs and EVs... 36
High-Side Automotive Battery Monitoring... 39
Current Sensing in an Automotive Environment... 42

SLEEPING CONSERVES ENERGY

How to reduce the power consumption of CAN networks using the Partial-Networking Mode

By: Fritz Burkhardt

Minimizing energy consumption has become a major factor for any new product design in recent years.

Hardly any industry can afford to disregard this issue in the definition, development, or marketing of their products and the automotive industry is no exception. Manufacturers have made significant efforts towards reducing fuel consumption by efficient engine management and weight minimization. Meanwhile, developers are focusing on the vehicle's electronic functions as well.

Until now, the use of low-power electronic-control units was particularly important for parked vehicles in order to achieve maximum standby times with existing battery capacities. In the meantime, however, current drain has become important for driving vehicles as well because the combustion engine must deliver the electrical energy with a direct influence on fuel consumption.

Comparatively low fuel consumption is a key selling point because it immediately affects operating costs for the car owner. Today, however, another factor complements this perspective.

The reduction of greenhouse-gas emissions, which are harmful to the earth's climate, has been the goal of many initiatives of the international community. Consequently, the European Parliament passed a regulation stating mandatory limits for the CO_2 emissions of new vehicles. The regulation fixes severe penalties for violating these limits to ensure that car manufacturers assume their responsibility to reduce their products' energy consumption.

The e-mobility trend may emerge as an additional motivation in the future: Minimizing energy consumption will become more and more important in electric vehicles whose operating range will be a significant factor for this technology's acceptance.

Apart from factors including engine efficiency, vehicle weight, and aerodynamic drag, the power efficiency of the electronic control units is a wide field of activity for designers willing to save energy.

Analyzing the electronics landscape in modern vehicles quickly yields several observations: The vehicle does not require all of the functions that the many control units offer all the time and in every driving situation. The continuous current drain these modules impose isn't, therefore, always necessary. This is particularly true for convenience functions including seat electronics, trailer-control units, or tailgate-control units because these functions only rarely operate or because they are not necessary all the time. Additional examples include door-control units, auxiliary heating, sunroofs, and rear-view cameras. On the other hand, it must be possible to activate these control units at any time in order to avoid any functional or convenience impairment.

For example, assume an average current drain of 100 to 150 mA and a battery voltage of 14 V, potential saving amounts to 1.4 to 2.1 W for each idling control unit. Total energy savings for 20 CAN nodes capable of partial networking therefore amount to an average of 35 W without any negative impact on functions or convenience features.

According to the established conversion formula, 40 W of electrical power represent 1.0g of CO_2 emissions per kilometer. Thus, the introduction of partial networking leads to potential emission reductions of 0.85 grams of CO_2 per km.

The aforementioned EU regulation stating a violation penalty of €95 for each gram of CO_2 per kilometer yields potential savings of approximately €80 Euros per vehicle for car manufacturers.

But there are even more reasons why designers should consider opportunities for partial networking. These includes the charging of electric vehicles. Although this requires a communication link to the supervising control unit, most of the control units that connect to the bus are not necessary for this task and thus the vehicle can selectively power them down.

The same is true for future application scenarios entailing data transmissions between a parked vehicle and mobile end devices. These future-use cases also result in increased requirements regarding the operating life of the components. Partial networking can compensate for this to a certain extent, resulting in reduced costs, which explains the industry's intensive efforts to exploit this potential.

At the Fachkongress Automobil-Elektronik, which took place on June 8, 2011 in Ludwigsburg, Germany, German OEMs jointly announced starting volume production of CAN partial networking in the short and medium term.

Although current CAN nodes already provide low-power modes, such as standby and sleep, they immediately wake up if any communication occurs on the bus. These low-power modes are thus only useful if all nodes on the bus disable simultaneously—a so-called bus idle— as is the case for a parked vehicle. When any message source transmits data on the CAN bus, transceivers wakeup all connected nodes. Consequently, individual control units cannot remain in sleep mode while communication on the bus is ongoing.

One suitable approach divides the network into sub-networks and disconnecting specific controllers from the supply voltage. Apart from the restrictions regarding the network layout, using multiple power supplies leads to additional overhead. Nonetheless, designs of

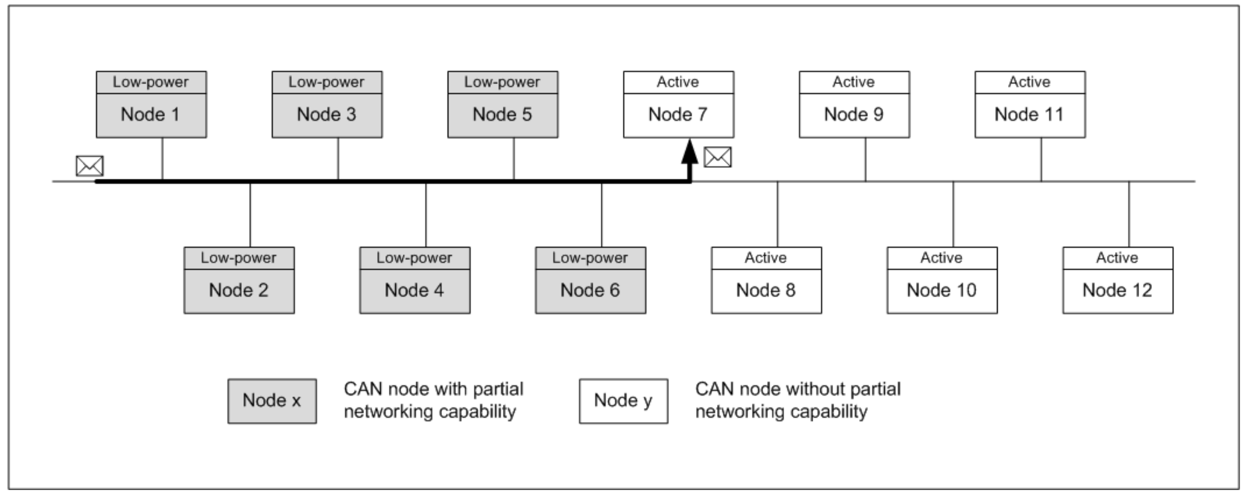

Figure 1: CAN network with partial-networking controllers during the transmission of a message to ECU7 (without partial-networking support)

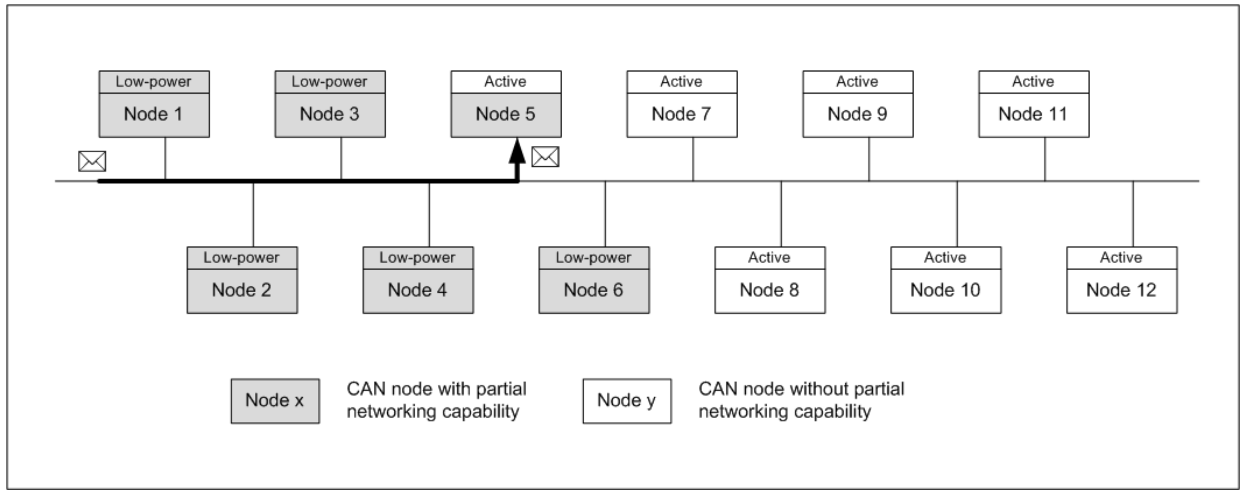

Figure 2: CAN network with partial-networking controllers during the transmission of a message to ECU5 (with partial-networking support)

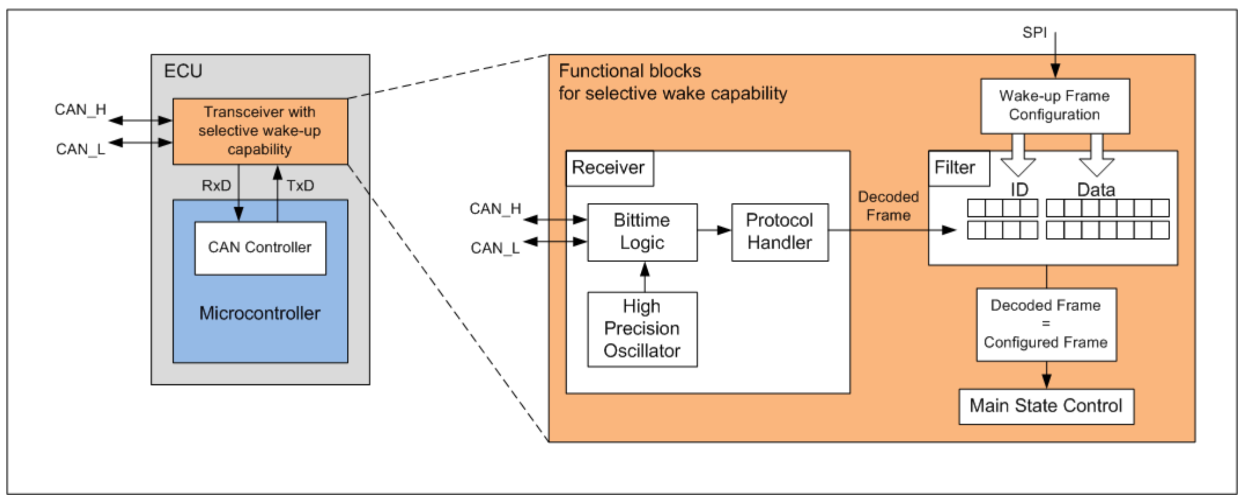

Figure 3: Functional blocks of a partial-networking transceiver

this kind are already in use today.

Obviously, the most flexible approach is to wake up specific nodes using dedicated, pre-defined wake-up messages. To support selective addressing, CAN controllers in a sleep or standby mode must be able to monitor CAN messages for previously-negotiated wake-up messages and to respond only if necessary.

Consider, for example, a network consisting of 12 nodes (Figure 1). Six nodes support partial networking while the remaining units use conventional transceivers without this capability. When the bus is active and a message addresses Node 7, Nodes 7-12 are active due to the ongoing bus communication while Nodes 1-6 remain in low-power mode because they did not receive a selective wake-up message.

Now consider a second scenario in which Node 5 receives a selective wake-up message (Figure 2). This node recognizes the wake-up request and enters active mode. Nodes 7-12 remain active also due to the ongoing bus communication while nodes 1-4 and 6 remain in low-power mode. Ideally, the detection of wake-up messages should occur in the transceiver because this is the only way to avoid activating the microcontroller with the resulting increased current drain.

The strength of conventional transceivers is their bus-level translation capability with full signal fidelity and immunity to external noise signals and bus interference. Having only very basic logic functions for detecting simple bus errors, every bus edge activates them. This, in turn, precludes capturing and evaluating any incoming messages because this is the task of the MCU's on-board CAN controller, which has the precise reference clock necessary for evaluating the message.

CAN transceivers capable of partial networking therefore need a highly precise internal reference clock in order to reliably capture and decode the incoming bitstream. In addition, this reference clock must be stable in the relevant temperature range. Considering the maximum tolerance of the transmitting node and common disturbances on the bus, including blurred edges, reflections, and EMI, the oscillator must provide precision of < 1% over the entire temperature range from -40 to +105 °C for the operating life of the component. The oscillator concept used in partial-networking transceivers therefore plays a primary role and represents the main challenge during the development of these devices.

The node must then extract the information payload from the bitstream according to the CAN protocol before the node can compare the data to its previously-configured wake-up message.

The transceiver must thus provide an interface for configuring the partial networking mode and the dedicated wake-up message (Figure 3).

As mentioned above, car manufacturers are working hard to bring partial networking into volume production. However, these efforts will only be successful if the industry can standardize transceiver features.

For this purpose, a working group called SWITCH (Selective Wakeable Interoperable Transceiver CAN Highspeed) is preparing a standardization proposal based on a relevant requirement specification. The proposal is currently under discussion with the International Standardization Organization to define a supplement for ISO 11898 (Road Vehicles – Controller Area Network CAN). STMicroelectronics is contributing to the definition of this functionality and is working on the implementation of suitable transceivers.

The company has worked closely with a major German car manufacturer, which is running in-vehicle tests on a first device. The company expects to be in volume production of the device in Q4 2012.

Fritz Burkhardt
Senior Technical Engineer, Marketing
STMicroelectronics

www.st.com

HALL-EFFECT CURRENT SENSING IN HEVs AND EVs

Wide bandwidth and inherent galvanic isolation simplify current measurements in demanding automotive applications.

By: Shaun Milano, Michael Doogue, and Georges El Bacha

Consumers are embracing environmentally friendly green cars due to the rising cost of fossil fuels and a growing concern for the health of the environment.

Sales forecasts predict that green cars will comprise 3% to 4% of all vehicle sales by the year 2016. After 2016, estimates call for a more rapid adoption of green cars, with green car market share ranging from 8% to 19% in 2021. The most popular green car, both today and in forecasts through 2021, is the HEV (hybrid electric vehicle).

HEVs employ complex power electronic circuitry to control the flow of electric energy through the vehicle. In a single motor HEV, the motor acts as a traction drive in parallel with the internal-combustion engine, or as a generator to charge the battery during regenerative braking. Both HEVs and EVs (electric vehicles) contain various systems that require electrical current sensors for maximally efficient operation, including AC-motor and DC-DC-converter applications.

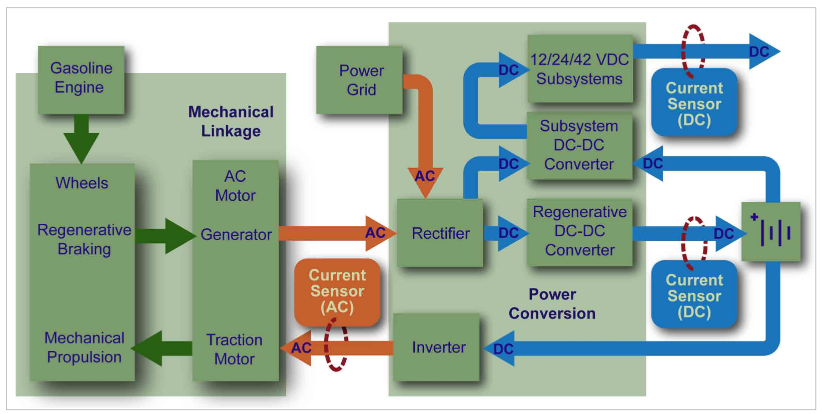

Figure 1: Typical HEV system block diagram.

The HEV Power Cycle

In the HEV power cycle the power converter inverts the main battery voltage and applies the resulting AC voltage to the traction motor, which in turn drives the wheels (Figure 1). During regenerative braking, the AC motor also serves as a generator. When the regeneration system is active, the power converter rectifies the output of the motor-generator to a DC voltage sufficient to charge the HEV battery cells, completing the power cycle. For EVs and plug-in HEVs, the power converter also rectifies the line voltage to charge the battery.

The regenerative braking process is a primary contributor to HEV's and EV's energy efficiency because the power converter partially recovers braking energy normally wasted in the form of heat, and uses it to charge the main battery. To power the low voltage infotainment and body-control subsystems in the car, a DC-DC converter reduces the battery voltage—typically 300 to 500 V—to a lower-level DC voltage.

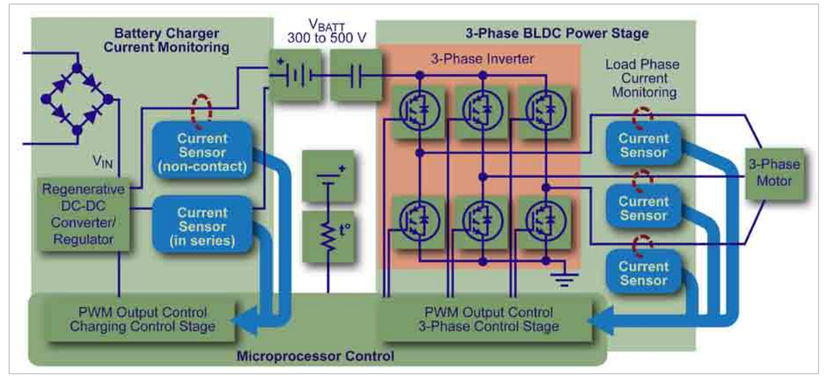

Figure 2: DC-DC converter charger (left) and 3φ DC-AC Inverter (right).

One drawback of conventional Hall-effect sensors in current sensing applications has been a general limitation in both accuracy and output signal bandwidth. Signal-processing and package-design innovations enable new Hall-effect current sensors with > 120 kHz output bandwidths, low output phase shift, high current resolution, and low noise spectral density.

Current Sensing in Inverter Applications

The driver in a typical inverter converts DC battery voltage to a 3φAC voltage that the traction motor requires for efficient operation (Figure 2). Current sensors measure the three inverter phase currents and, typically, a controller uses the resulting information to control the PWM inverter switches—usually IGBTs. The inverter control loop requires high-bandwidth current sensors to improve accuracy, maximize motor torque, and maximize overall motor efficiency. High-side current sensors with fast response times also enable over-current protection during short circuit conditions from a motor phase to the system-ground node.

For example, the Allegro A1360 linear Hall device meets the voltage isolation, > 200 A load current, and high-bandwidth demands of HEV inverter applications. The Hall-effect sensor IC typically locates in the gap of a ferromagnetic toroid which surrounds each inverter phase conductor in the motor (Figure 2). As current flows in the conductor, the toroid concentrates the resulting magnetic field through the SIP (single inline package) device. The transducer provides an output voltage proportional to the current. The device is available in a proprietary, 1 mm thick package that reduces eddy current losses to improve sensor output bandwidth when compared to conventional IC packages.

The A1360 and similar devices have a typical output bandwidth as high as 120 kHz and offer high-resolution high-accuracy performance that allow for high-speed control of the PWM switches in an inverter system. Additionally, these SIP sensors offer a 3 μs output response time for IGBT over-current protection applications. The form factor of this current-measurement circuit is also smaller than current transformers. Nonetheless, it provides the necessary galvanic isolation because the sensor IC output leads do not connect to the high-voltage current-carrying conductor in each of the motor's phases.

Electric Motor Control

A prominent trend for improving energy efficiency in HEVs and EVs (and, to a lesser extent, in internal-combustion engines with idle-stop capability) has been the conversion of belt-driven and hydraulic actuators to electrically-driven actuators. For instance, in traditional internal combustion engines a fan belt drives the cooling fan, which operates continuously while the engine is running. The same applies to power-steering pumps and other belt-driven loads.

Replacing belt-driven actuators with electric motors improves energy efficiency and allows for greater control of the actuators. Precision, high-speed current-sensor ICs provide the bandwidth, response time, and accuracy performance necessary to optimize motor performance but must meet qualifications for the demanding under-hood environment.

DC-DC Converters

The current sensing range and the isolation voltage determine the optimum current-sensor IC package for use in DC-DC converters. Current sensors in DC-DC converters often must sense current in a spectrum that includes DC. This requirement precludes current transformers in fully optimized systems. Using shunt resistors in these applications is also challenging because the high input or output DC voltages require expensive, high-common-mode input operational amplifiers. A Hall-effect sensor with inherent galvanic isolation, wide current bandwidth, and a transduction response that extends to DC is a logical choice for DC-DC converter applications in HEVs.

A regenerative converter uses a current-sensor IC that can operate at traction-battery voltages. Accurately sensing the converter output current is a critical function because correctly metering the charge current that the converter delivers to the HEV battery extends its operating life.

The ACS714, for example, is a current-sensor IC suitable for many lower current, subsystem DC-DC converter applications. The ACS714 is a factory-trimmed, galvanically-isolated sensor IC available in an extremely small form factor SOIC-8 package with an integrated 1.2 mΩ conductor for low power loss. For higher-current applications, current sensor ICs such as the Allegro ACS758 incorporate a 100 µΩ conductor and a ferromagnetic core into a small form factor galvanically-isolated package capable of sensing 50 through 200 A. For greater measurement ranges, the SIP based toroid configuration mentioned earlier can sense currents above 200 A.

Shaun Milano, Strategic Marketing Manager

Michael Doogue, Director,
Linear and Current Sensor Business

Georges El Bacha, Systems Engineer

Allegro MicroSystems
www.allegromicro.com

HIGH-SIDE AUTOMOTIVE BATTERY MONITORING

Assessing battery charge and health depends on synchronized measurements of voltage, current, and temperature.

By: Manfred Brandl

Manufacturers are electrifying more functions within a car, reducing the mechanical load on the internal-combustion engine.

These functions include water, oil, and fuel pumps; valve actuation; and power steering, in addition to safety, navigation, and infotainment systems. As the power load shifts from the engine to the vehicle's battery, the requirement to keep the battery charged and functioning correctly becomes even more critical. Designers are requiring better battery management capabilities to monitor and distribute power.

SoC (State of Charge) and SoH (State of Health) are two key attributes of lead-acid batteries that battery sensors monitor. SoC, which indicates how much charge the battery can deliver, is expressed as a percentage of a battery's rated capacity. SoH indicates how much charge the battery can store. To compute these values, a monitoring system measures the battery's current, voltage, and temperature and sends these data to a microcontroller. The microcontroller filters the battery data, computes the SoC and SoH, and sends the results to the ECU (electronic control unit) via the industry standard LIN communications interface.

A battery sensor must simultaneously measure the battery's current and voltage. Excellent accuracy is required for SoC measurement and to track dynamically the battery impedance. The monitoring system must make these measurements often, typically at a rate of 1 kHz, with the current and voltage measured simultaneously and with virtually no insertion loss. Key attributes of this measurement system are very low noise, high linearity, and zero offset. Additionally, the system makes all measurements under the harsh conditions of an automobile engine compartment.

Traditionally, battery sensors were designed to be placed at the negative pole of the battery. However, there are benefits to configuring the sensor for high side measurements. This would provide the ability to place the sensor apart from the battery in the junction box, reducing demands on form factor and mechanical rigidness, which is the most significant cost driver when the sensor is located at the battery pole. Manufacturers could also combine a high-side sensor with a junction box module, which addresses functional safety. This is becoming increasingly important when sharing a microcontroller—another opportunity to reduce cost. This would also support the trend to design vehicles with fewer, more centralized ECUs.

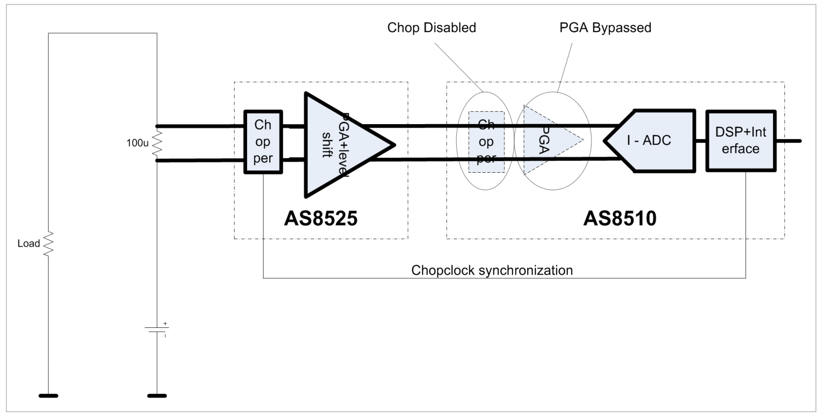

Figure 1: Functional blocks for ams's two-chip sensor interface for high-side automotive battery current sensing.

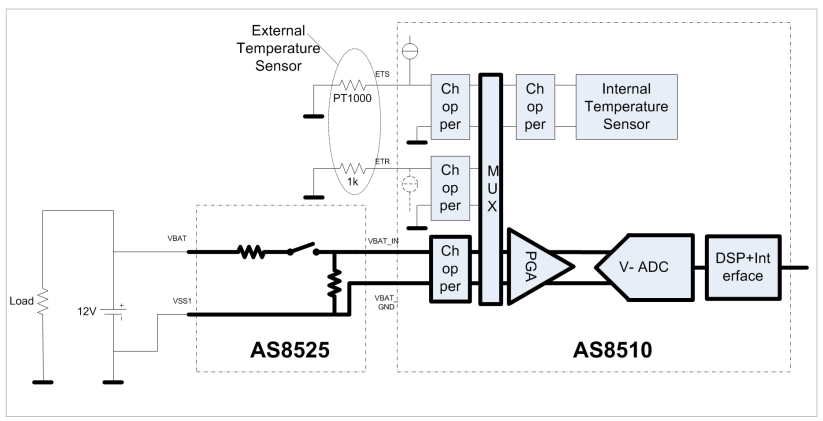

Figure 2: Block diagram showing the voltage sensing function in a high-side automotive battery sensor.

An example of a high-side battery sensing system includes the ams AS8510 Data Acquisition Front End and the AS8525 High-Side Current Sensor Companion IC. It uses a 100-μΩ shunt at the battery's high side to measure currents ranging from 1 mA to more than 1 kA with negligible insertion loss. It enables stand-by current, voltage, and temperature monitoring modes at very low current draw of around 80 μA – a crucial requirement in automotive battery sensors. The system's output can route to an existing ECU, thus reducing BOM cost.

Shunt resistor specification
Current sensing requires the use of a low-insertion-loss 100-μΩ shunt connected to the positive battery terminal in series with the load (Figure 1). The temperature drift at the shunt resistor must be extremely low, as any drift in the resistance value of the shunt directly affects the current readings generated by the sensor.

For the resistive element, ams recommends a 100-μΩ BAS shunt with Manganin alloy. Its temperature coefficient is low, and its Seebeck coefficient is similar to that of copper. This means that the signal generation attributable to thermocouple effects when inserted into a copper rail is negligible. The shunt's change in resistance value over time is also both minimal and predictable.

Wide measurement range
The system measures current over a range of 1 mA to 1 kA. This requires a sensor interface with a measurement range of > 100 mV, and a resolution of better than 1 μV. The system implements auto zero offset by a sequence of signal-conditioning functions: chopping the analog sensor signal, amplifying and level-shifting the signals, digitizing them, and de-chopping in the digital domain. The architecture enables cancellation of the offset and the low-frequency noise components of the entire measurement path.

In this example, the analog signal chopper receives the shunt signal at a nominal 14 V common-mode input voltage. The signal processing chain amplifies and level shifts the chopped signal to a low common-mode voltage and forwards the result to the AS8510's ADC.

Voltage Measurement
To make voltage measurements, a precision resistive divider inside the AS8525 attenuates the battery voltage, which then connects to the second data acquisition channel of the AS8510 as a differential signal (Figure 2). The system can multiplex this channel with input channels for either an external or internal temperature sensor.

Temperature Sensing
If the battery sensor is placed at the battery terminal, the AS8510's internal temperature sensor can be used to pick up the battery temperature through the terminal, shunt, and PCB. If the sensor's electronics are located away from the battery in a separate compartment, the system can use an external temperature sensor to measure the battery's temperature.

The common-mode input signal produces current measurement errors of typically 0.05% per Volt. As the common-mode input signal for the shunt is the same as the battery voltage, and the system measures the battery voltage in sync with the current, this error is correctable in software in the external microcontroller. An end-of-line calibration procedure can capture an accurate value for the common-mode error: Apply a reference current at two different common-mode shunt voltages, measure the deviation, and store this value as the calibration factor.

Manfred Brandl
Product Manager, ams AG

www.ams.com

CURRENT SENSING IN AN AUTOMOTIVE ENVIRONMENT

With many competing sensing technologies, designers must pick the attributes most important to each application.

By: Warren Pettigrew

The Automotive industry has long been the ultimate test ground for electronic components.

Few terrestrial environments present such a combination of demands as does the under-hood locale with its operating temperature range, mechanical shock and vibration, and electrically noisy environment. Above all, automotive electrical sensors must perform consistently well at cost points measured in tenths of a cent.

Modern expectations of current sensors are very different from what they were even five years ago. As complexity grows, performance and reliability must increase disproportionally because of the challenge of repair and service in the field. This is particularly true in the electric-vehicle market, where many current sensors are now required to allow the management of routine (and not so routine) operations. It is just not practical to train vast numbers of service technicians. It is far better not to have failures, so repair and service is no longer a requirement.

Another relentless expectation is cost reduction. The market disproved the old adage that you can have either "high quality or low cost, but not both" long ago. Automotive customers demand both and this does create challenges:

Operating conditions

Low voltage supplies are really the only option – typically 5 or 3.3 V. but not both to avoid the cost of dual supplies. Low quiescent power is also necessary to reduce power supply cost and bulk. This virtually eliminates power hungry closed-loop current sensors, which carry a cost premium as well. In some environments, sensors need immunity to large supply transients, which significantly complicates sensor power-supply design.

Commonly, carmakers demand a -40 °C to +125 °C operating temperature range. This range requires that sensor makers carefully select materials and components for a sensor assembly. Magnetic field sensors must remain stable and the magnetic circuit must have stable characteristics over its operating flux range.

Mechanical configuration

In many applications, sensors mount in free air outside of any electronic enclosure. For these cases, sensors need to be water proof probably to an IP65 rating as well as mechanically robust. Many times customer-specific mounting is necessary along with an automotive style waterproof connection. Significant tooling and product design is therefore necessary to satisfy all interested parties.

Designers must consider the cost of any additional components or space and include them into the cost of current sensing. Non-intrusive mounting is always preferable, especially for externally mounted sensors. Clips are preferable to screws. Screw heads, if present, must be readily accessible and, more recently, the use of an Automotive Industry standard Adhesive Transfer Tape mounting system permits reliable fixing with one sided access. The final installation must comply with shock and vibration requirements. Cables must route to protect from snagging, vibration, excessive heat, and corrosive fluids.

Under-bonnet space is always a premium so size and weight are important quantities. Energy efficiency is steadily increasing in importance with each rise in the price of oil. Weight is doubly important for EVs as this reflects in the size and cost of the battery. Energy consumption relates directly to weight so carmakers count even small components. Where high currents are present, it is a real challenge to develop light-weight sensors.

Current range:

Where it is necessary to measure battery current, system designers often need to know both the peak discharge current - which may be many hundreds of amps, as well as the current at charge completion, which could be a fraction of an amp. No one economical sensor technology can presently perform over this span, so a hybrid of sensor types is necessary. This generally requires having a low-current sensor that is not corrupted by high currents in combination with an economical high-current sensor that also has good low-current performance.

Apart from the challenge of measuring current over such a wide dynamic range, there is the challenge of measuring the sensor output over that range. Measuring milliamps to hundreds of amps has a span of say 100,000:1. If an ADC were to read this signal, it would need 17 bits resolution. This is obviously not practical, so again we see the need to split the range into two or three subranges.

Stability

Since the sensors have to operate over a very wide temperature range, their gain and offset need to be very stable. It is necessary to assess the effect of system performance with calculated drifts.

Another important parameter if sensing low DC currents is the sensor's residual offset after a high DC load due to core remanence. This offset is generally in the order of 0.5A so accuracy below 1A will be very poor. There are very special low remanence core materials available, or degaussing may be an option, but these features add cost.

In systems that implement cycle-by-cycle current control, the current sensor frequency response needs to be greater than 4X the fundamental frequency of the switching control system. Where the current sensor is to protect against overloads or short-circuits, its reaction speed needs to be matched against the likely rate of rise of current and the circuit tolerance to short-term overload. Fortunately, currents don't rise instantaneously—$V/L = dI/dt$—and there is always some parasitic inductance: As a rule of thumb, a conductor has about 1 nH/mm inductance—less for bus bar, more for PCB traces.

Voltages in HEV applications are creeping up, and so the isolating ratings of sensors must follow, with proper safety margins. Voltage ratings drive creepage and clearance dimensions—minimums for which standards provide.

Sensors must also withstand and operate to specification under extremes of temperature and humidity, water-blasting, aggressive fluids, high vibration and shock, large electrostatic fields, large magnetic fields, and high electromagnetic fields. There are standards that define all of these under-hood environment factors. Still sensor providers and automakers must agree on the complete set of environmental conditions.

Sensor technologies

Where galvanic isolation is not

Technology	Offset Stability	Gain Stability	Span	Linearity	Hysteresis Error	Stray Flux Immunity	Quiescent Current	Frequency Response	Ambient Temp Range	Overload Capability	Size	Price
Core-less open-loop	P	M	G	G	Ex	P	VG	G	VG	M	Ex	Ex
Ferrite core open-loop	P to G	M	G	M	G	M	VG	G	VG	Ex	Ex	VG
Iron core open-loop	P to G	M	VG	G	VG	G	VG	G	Ex	Ex	VG	G
Closed-loop	VG	Ex	VG	Ex	VG	VG	P	VG	M	G	M	M
Low-current shunt	Ex	Ex	VG	Ex	Ex	Ex	Ex	Ex	Ex	G	G	Ex
High-current shunt	VG	Ex	VG	Ex	Ex	Ex	Ex	VG	VG	M	M	G
FET on resistance	VG	P	P	P	Ex	Ex	Ex	VG	G	M	Ex	Ex
Shielded air-core open-loop	G	G	Ex	VG	Ex	VG	VG	Ex	Ex	Ex	Ex	Ex

Table 1

necessary, shunts become an option. For low currents, they are attractive, but as currents get above 100 A or so, their bulk and cost grows exponentially. Larger shunts are also problematic for measuring high frequencies as their inductance causes inductive kicks of considerable magnitude.

Sensor makers can manufacture low-current coreless open-loop hall-effect sensors in IC form so these can be low cost and do have their place for some applications generally in the 20A to 50A current range. The lack of core means lack of shielding against stray magnetic fields. Using a pair of hall sensors and making a differential measurement improves immunity to stray fields. However, the lack of a magnetic circuit to amplify flux strength does mean field strengths are low so sensitivities need to be set high, making this type of sensor vulnerable to drifts.

Open-loop hall-effect sensors have good all around performance. Sensor manufacturers can select components such as core material and hall sensor to optimize performance for a particular application. Improvements in hall-sensing technology now allow these sensors to perform like some

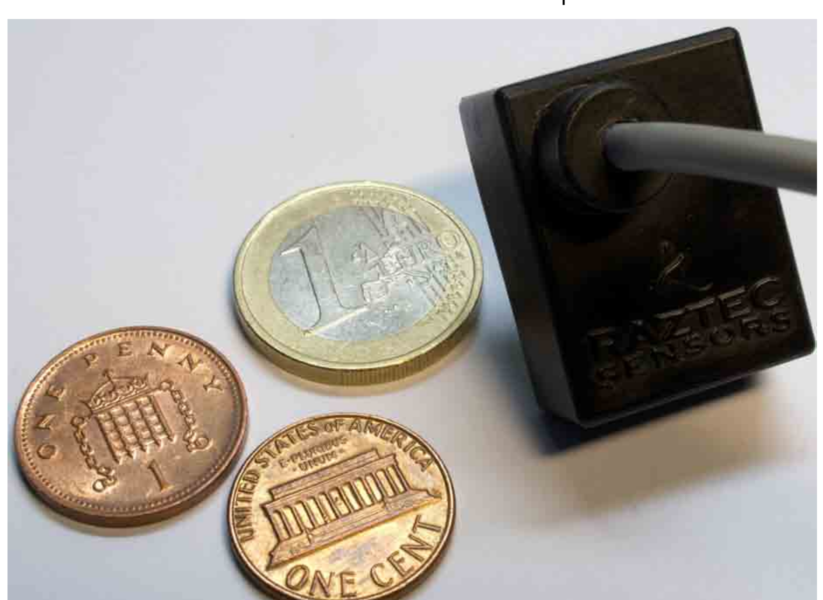

Figure 1: An example of a shielded air-core open-loop current sensor from Raztec provides a strong combination of high performance in a small package and at low cost.

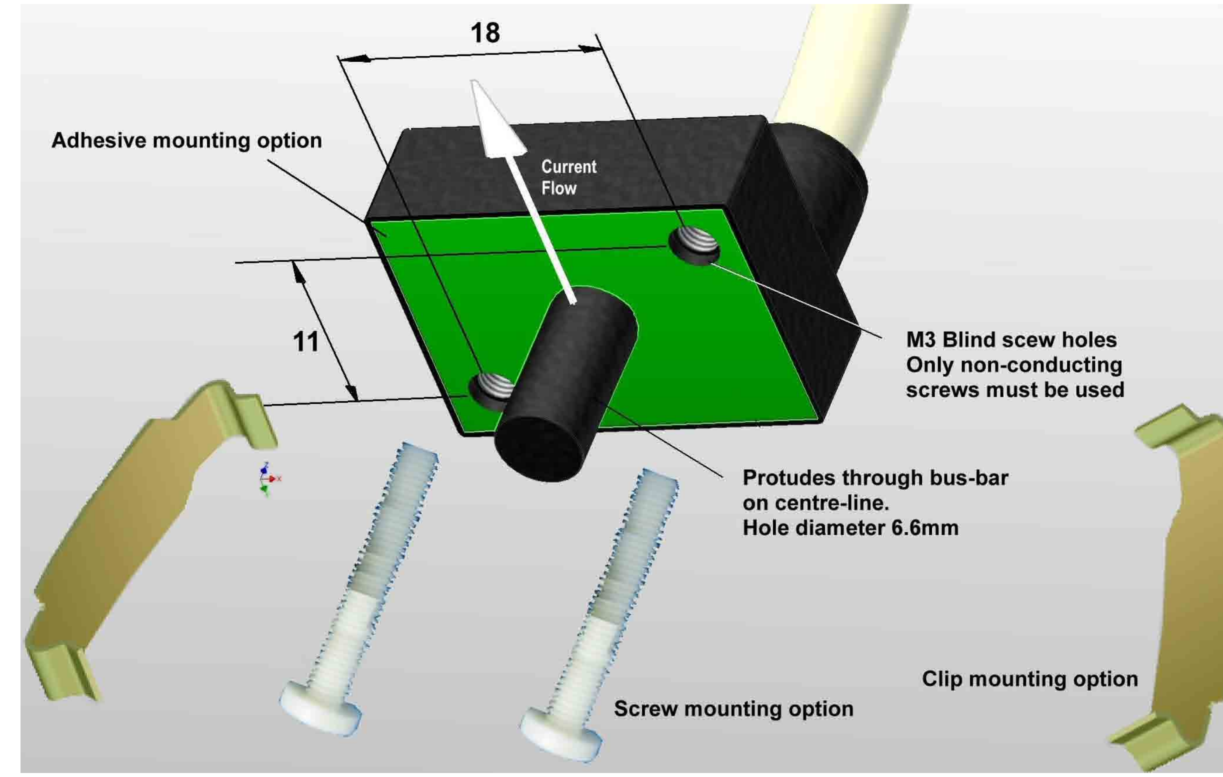

Figure 2: The shielded air-core open-loop current sensor also provides for several mounting options, simplifying design in.

closed-loop technologies.

The necessary compensating coil and its driving electronics add bulk and cost to closed-loop hall-effect sensors, but do allow for excellent gain stability and speed of operation. Because of their inherent shortcomings however, these sensors are not commonly used in an automotive environment.

Measuring current through a FET's on resistance is a sensing option where precision is unimportant and low cost is a premium. The method is software intensive and needs a capable micro for signal processing. Thermal drifts are a menace and in-process calibration is essential but the result is nearly free.

Shielded air-core open-loop high-current sensors take advantage of significant improvements in hall-effect devices, opening the way for precise direct differential sensing of current generated magnetic fields. Differential field sensing provides immunity to common-mode fields. Screening provides immunity to primary-generated electrostatic fields. Hybrid techniques improve frequency response. The significant benefits of this technology are its ease and flexibility of mounting and its small size (Figures 1 and 2). The sum of qualities very much aligns this technology to automotive needs.

A summary of these various sensing technologies appears in Table 1. There, the grading are Ex—excellent, VG—very good, G—good, M—modest, and P—poor.

Warren Pettigrew
Chief Technology Officer
Raztec Sensors

www.raztec.co.nz

VEHICLE ELECTRIFICATION SPARKS ENGINEERING DEMAND

By: David G. Morrison

Though electric vehicles (EVs) and hybrid electric vehicles (HEVs) only account for a modest percentage of overall car sales, the sales of these more-electric vehicles are on the rise. According to a forecast by Pike Research, annual sales of EVs and HEVs will reach 2.9 million vehicles by 2017.[1]

Meanwhile, vehicle electrification is also taking root in the commercial and industrial markets. For example, another firm, IDTechEx, predicts that sales of heavy industrial vehicles like cranes and forklifts will grow nearly 70% over the next five years, reaching 763,000 vehicles in 2017 (Table 1.)[2] These growing EV and HEV markets have been creating numerous design challenges and career opportunities for power electronics (PE) engineers, as documented in prior articles.[3,4,5,6] But one issue that may have received little attention previously is how these design challenges and opportunities are cropping up in various segments of the automotive industry and at different points in the supply chain.

A recent survey of automotive industry websites reveals job opportunities in several types of companies. You can view a listing of these job openings in the online version of this article. As might be expected, there are opportunities for PE engineers at the larger, more-established automotive companies such as Ford and the tier 1 suppliers such as Delphi and Continental. But there are also a number of opportunities for PE engineers at EV specialist companies such as Tesla Motors, VIA Motors, and GreenTech Automotive. Similarly, there are companies specializing in electric power train and propulsion technology such as Mission Motors and AC Propulsion that seek experienced PE engineers.

But there's also another dynamic segment of this industry that needs power electronics expertise—the battery companies who are developing the advanced cells, packs, and systems that will be critical to the success of new EV and HEV designs. These companies need EEs with various PE skills to address battery management issues and develop related hardware. The list of these companies currently seeking EEs includes the likes of Dow Kokam, Sion Power, Valence Technology,

Vehicle type	Unit sales	
	2012	2017
Heavy Industrial (includes mobile cranes, forklifts, and trucks)	453,000	763,000
Buses	22,000	58,000
Light Industrial/Commercial (catch-all category that includes a golf carts, airport baggage transports, lawn mowers, and many other miscellaneous types)	263,000	333,000

Table 1. Current and projected sales of commercial and industrial electric and hybrid-electric vehicles (Data courtesy of Dr. Peter Harrop, Chairman of IDTechEx.)

them at an affordable cost. If you're going to convert a large percentage of the vehicles produced into electric drive power

and Johnson Controls.

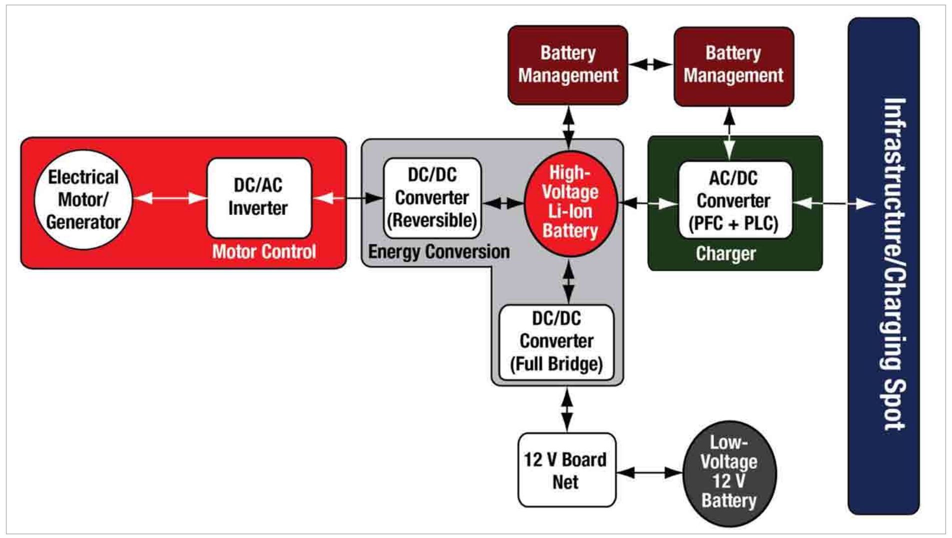

Figure. An example power system architecture for a hybrid electric vehicle. (Courtesy of Texas Instruments.)

Regardless of where engineers are in the automotive supply chain, there is an imperative to develop solutions at the lowest possible cost. This goal takes on even greater significance in the development of EVs and HEVs, since the industry is trying to reduce the price premium associated with these vehicles. Naturally, this issue impacts the design of all the power electronics functions.

Table 1. Current and projected sales of commercial and industrial electric and hybrid-electric vehicles (Data courtesy of Dr. Peter Harrop, Chairman of IDTechEx.)

Gary Cameron, currently Director—Advanced Electronic Controls Engineering at Delphi, has pointed out that the techniques for managing power in electric and hybrid-electric vehicles are understood, but the cost of implementing the various power conversion and power management functions needs to be driven down.

"The big challenge is doing trains, you've got to get the cost closer to parity with the alternatives. They continue to make improvements in internal combustion engines, diesel, gas, etc. but they're still going to need electrification. The overall car can't be too expensive for the public to buy," says Cameron.

Technology Developer	Partner	Description	Type
A123	Fisker	A123 has invested $23 million in Fisker and will supply batteries as well.	PHEV
NEC	Nissan	Supply packs for PHEV, HEV, and EV.	P/H/EV
Argonne National Laboratory (ANL)	LG Chem, GM, Toda Kogyo, BASF, Envia Systems	ANL has licensed its composite NMC cathode material to numerous corporations.	P/H/EV
BYD	Daimler	BYD and Daimler formed a joint venture called Shenzhen BYD Daimler New Technology to develop an EV for the Chinese market.	EV
Envia	General Motors	GM Ventures invested $7 million in Envia.	--
GS Yuasa	Mitsubishi; Honda	GS Yuasa and Mitsubishi formed a joint venture to produce Li-ion batteries called Lithium Energy Japan; GS Yuasa and Honda formed a joint venture to produce Li-ion batteries for HEVs.	EV; HEV
JCI-Saft	Ford	JCI-Saft supplies batteries to Ford for a PHEV.	PH/EV
LG Chem	Eaton, Ford, GM, Hyundai, Volvo	LG Chem has secured numerous supply relationships for vehicles across the spectrum.	P/H/EV
Panasonic	Toyota	Panasonic and Toyota formed a joint venture called Primearth EV Energy to create battery packs for Toyota.	P/H/EV
Sanyo	Audi, Volkswagen, Suzuki	Sanyo has supply contracts with multiple OEMs for Li-ion batteries.	P/H/EV
SB LiMotive	BMW, Chrysler, Volkswagen	SB LiMotive is a 50:50 joint venture between Samsung SDI and Bosch, and has secured supply relationships with multiple automakers.	EV
Shin-Kobe	Hitachi	Hitachi and Shin-Kobe formed a JV Hitachi Vehicle Energy that will supply batteries for 100,000 GM HEVs through 2015.	HEV
Toshiba	Mitsubishi	Toshiba will supply its SciB batteries to Mitsubishi for its Minicab i-MiEV	EV

Table 2. Key Partnerships in Electric Vehicles (Source: Lux Research).

Fig. 1 shows the block diagram of an example power system architecture in a hybrid electric vehicle,[7] identifying the key power functions that PE engineers are working to develop with low-cost and other performance goals in mind.

In this diagram, the main traction battery is depicted in red, looking like the very heart of the system that it is. Perhaps, then, it is not surprising the amount of industry attention that is now focused on advanced battery development, which is evidenced by the numerous partnerships between automakers and battery developers. The chart in Table 2, provided by Lux Research,[8] highlights the various industry alliances to develop better, more-economical batteries for electric vehicles and hybrids. These alliances also suggest potential sources of employment, now or in the future, for PE engineers looking to play a role in putting more EVs and HEVs on the road.

About the Author

When he's not writing this career development column, David G. Morrison is busy building an exotic power electronics portal called How2Power.com. Do not visit this website if you're looking for the same old, same old. Do come here if you enjoy discovering free technical resources that may help you develop power systems, components, or tools. Also, do not visit How2Power.com if you fancy annoying pop-up ads or having to register to view all the good material. How2Power.com was designed with the engineer's convenience in mind, so it does not offer such features. For a quick musical tour of the website and its monthly newsletter, watch the videos at www.how2power.com and http://www.how2power.com/newsletters/.

David G. Morrison
Editor-in-Chief
how2power

How2Power.com


PSD
CHINA : NORTH AMERICA : EUROPE
Power Systems Design: Empowering Global Innovation
WWW.POWERSYSTEMSDESIGN.COM


Should a magazine website help you navigate the maze of technical resources on the Internet?
...acquaint you with experts in your field?
...provide insights on your career opportunities?
Should it be free?
explore
www.HOW2POWER.com
.COM
HOW2POWER
Answering Your Questions About Power Design

COMETH THE HOUR, COMETH THE MAN

By: Gail Purvis, Europe Editor, Power Systems Design

When BASF, Bosch, Merck, and Schott throw a combined weight and €300M in funding behind the German Ministry of Education & Research energy self-sufficient homes OPV (organic photovoltaics) project, it is worth watching.

When BASF, Bosch, Merck, and Schott throw a combined weight and €300M in funding behind the German Ministry of Education & Research energy self-sufficient homes OPV (organic photovoltaics) project, it is worth watching.

When that combines with the 2012 'Umsight' science award to Dr Jan Meiss for "New material concepts for organic solar cells," in cooperation with Heliatek GmbH and Fraunhofer IPMS – COMEDD achieving "an organic solar cell with 4.9% efficiency and 20% transmission," both the hour and the man have arrived.

As iconic older solar energy companies expire, rising star is Dresden-based OPV Heliatek GmbH in whom both BASF Venture Capital and Robert Bosch are investing φ.6m.

Low temperature (< 400°C) technology, cost-saving materials, a solar cell thinner than 500 nanometers, using carbonate dyes promises to yield light-weight, thin, rollable, plastic foil active cells, weighing 500 g/m2.

Keeping nextgen PV competitive, Switzerland's EMPA labs led by Ayodhya Tiwari has gathered up 12 university, research, and industrial organisations in the more modestly φom funded SCALENANO project. The aim is to scale-up materials and processes for low-cost, high-efficiency chalcogenides ($Cu_2ZnSn(S, Se)_2$-based absorbers, kesterites) using cheap, abundant materials.

It has three years to develop vacuum-free, electro-deposition processes for nanostructured precursors, industry players being Merck KGaA (chemicals), NEXCIS (photovoltaics), IMPT (TFT) and Hungary's Semilab (metrology).

It's going to be an energetic race to that grail of PV efficiencies and longer cell life.

www.powersystemsdesign.com

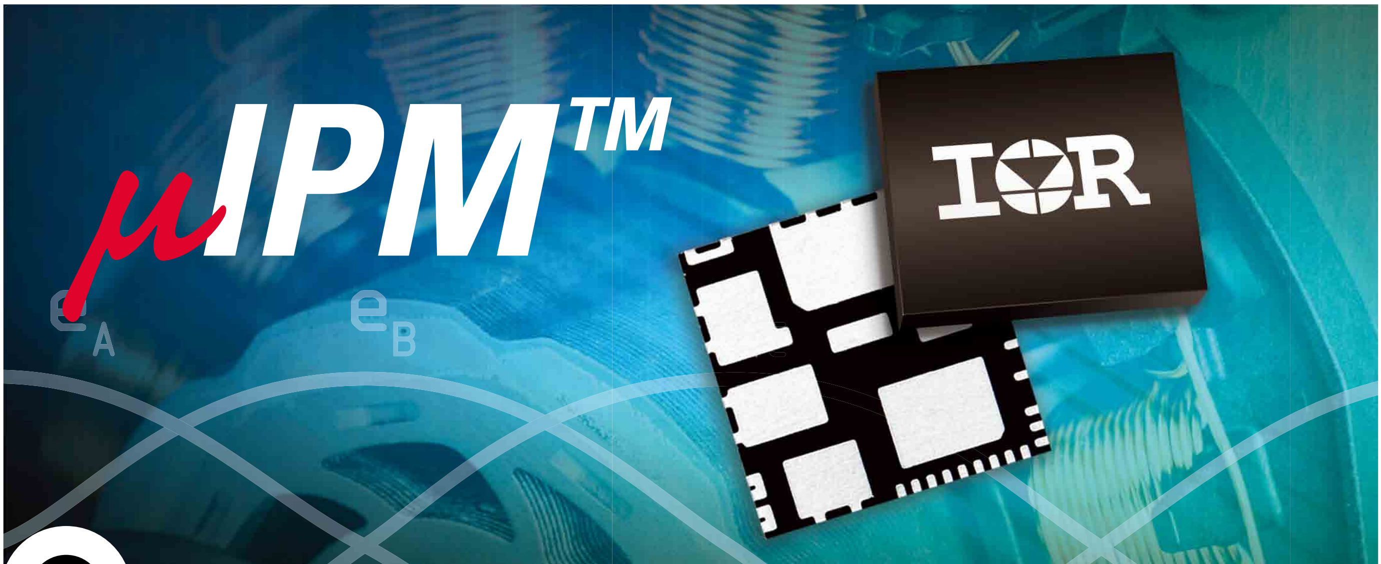

Innovative Power Module Reduces System Size

μIPM™ Power Modules Deliver up to 60% Smaller Footprint

Specifications:

Part Number	Size (mm)	Voltage	IO (DC@ 25°C)	Motor Current**		Motor Power VO=150/75VRMS	Topology
				w/o HS	w/o HS		
IRSM836-024MA	12x12	250V	2A	470mA	550mA	60W/72W	3P Open Source
IRSM836-044MA	12x12	250V	4A	750mA	850mA	95W/110W	3P Open Source
IRSM836-025MA	12x12	500V	2A	360mA	440mA	93W/114W	3P Open Source
IRSM836-035MB	12x12	500V	3A	420mA	510mA	108W/135W	3P Common Source
IRSM836-035MA	12x12	500V	3A	420mA	510mA	100W/130W	3P Open Source
IRSM836-045MA	12x12	500V	4A	550mA	750mA	145W/195W	3P Open Source

Features:

- 3-phase motor control IC
- 12x12x0.9mm PQFN package offers up to 60% smaller footprint
- Eliminates the need for heat sink
- DC current ratings from 2A to 4A
- Voltage range of 250V – 500V

μIPM™ Advantages:

- Shortens design time
- Shrinks board space requirements
- Simplicity - Eliminates Heat Sink
- Replaces more than 20 discrete parts to deliver a complete motor drive stage
- Slashes assembly time and cost
- Simplifies procurement and inventory management
- Reference design kits available for quick evaluation on any 3-phase motor

iMOTION™*

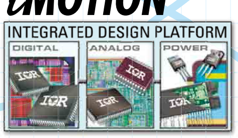

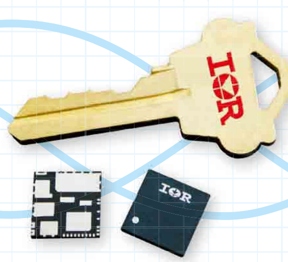

for more information call 1.800.981.8699 or visit us at www.irf.com

International IOR Rectifier
THE POWER MANAGEMENT LEADER

* IR's iMOTION™ (ai mo shan), representing the intelligent motion control, is a trademark of International Rectifier
** RMS, Fc=16kHz, 2-phase PWM, ΔTCA=70°C, TA ≈ 25°C